

Multi-study factor regression model: an application in nutritional epidemiology

Roberta De Vito*

Dept. of Biostatistics, School of Public Health, Brown University,
Providence, RI

Data Science Initiative, Brown University, Providence, RI

and

Alejandra Avalos-Pacheco

Applied Statistics Research Unit, TU Wien, Vienna, Austria

Harvard-MIT Center for Regulatory Science, Harvard University, Boston,
MA

April 27, 2023

Abstract

Diet is a risk factor for many diseases. In nutritional epidemiology, studying reproducible dietary patterns is critical to reveal important associations with health. However, it is challenging: diverse cultural and ethnic backgrounds may critically impact eating patterns, showing heterogeneity, leading to incorrect dietary patterns and obscuring the components shared across different groups or populations.

*Acknowledgments: RDV was supported by the US National Institutes of Health, NIGMS/NIH COBRE CBHD P20GM109035. This Manuscript was prepared using HCHSSOL Research Materials obtained from the NHLBI Biologic Specimen and Data Repository Information Coordinating Center and does not necessarily reflect the opinions or views of the HCHSSOL or the NHLBI. The authors would like to thank David Rossell and Giovanni Parmigiani for their precious advice.

Moreover, covariate effects generated from observed variables, such as demographics and other confounders, can further bias these dietary patterns. Identifying the shared and group-specific dietary components and covariate effects is essential to drive accurate conclusions.

To address these issues, we introduce a new modeling factor regression, the Multi-Study Factor Regression (MSFR) model. The MSFR model analyzes different populations simultaneously, achieving three goals: capturing shared component(s) across populations, identifying group-specific structures, and correcting for covariate effects.

We use this novel method to derive common and ethnic-specific dietary patterns in a multi-center epidemiological study in Hispanic/Latinos community. Our model improves the accuracy of common and group dietary signals and yields better prediction than other techniques, revealing significant associations with health.

In summary, we provide a tool to integrate different groups, giving accurate dietary signals crucial to inform public health policy.

Keywords: Factor analysis, Joint analysis, ECM algorithm, Nutritional epidemiology, Dietary patterns

1 Introduction

The impact of diet on diseases such as cancer (Willett and MacMahon, 1984), obesity (Foster et al., 2003) and cardiovascular disease (Kromhout, 2001; GBD 2013 Risk Factors Collaborators and others, 2015), has continually affected the world, including the United States, accounting for over 500,000 deaths annually, with 280,000 of those deaths due to obesity (Aune et al., 2016). Therefore, detecting eating patterns is crucial to assess the association between diet and diseases to guide and inform public health policy.

Diverse cultural and ethnic background components may have crucial impacts on eating patterns. In nutritional epidemiology, heterogeneous high-dimensional data coming from different populations or ethnic backgrounds (Stearns et al., 2017; Zulyniak et al., 2017) often arise (Haines et al., 1999), providing an opportunity to estimate shared dietary patterns and differences across them, leading to a better understanding of their association with certain types of diseases.

When analyzing different populations or groups, some diets and foods are reproducible and shared, while other diet characteristics are specific to each population. To handle this task, standard procedures involve stacking all the populations and performing traditional techniques such as factor analysis (Haines et al., 1999; Schulze et al., 2003; Edefonti et al., 2012; Bennett et al., 2022) to estimate dietary patterns, or performing factor analysis in each population and then adopting a measure of correlation to identify the most similar dietary patterns across the different populations or subgroups (Castello et al., 2014; Castelló et al., 2022). However, identifying dietary patterns in different populations can be challenging, mainly due to the diversity of ethnicities and demographic compositions among populations. Consumption patterns of foods, recipes or beverages can vary significantly between populations, critically affecting the risk of disease outcomes. Population-based

identification of these diets is crucial to provide essential knowledge and information for broad public health policies. However, distinctly unique populations can impact and mask the shared and reproducible dietary patterns among all the populations. Therefore, there is a crucial need for rigorous statistical techniques to identify concurrently common and study-specific diet characteristics to clearly estimate the association between diet and diseases.

Currently, researchers in the field are focused on identifying group or reproducible signal patterns. A recent development in this direction is the multi-study factor analysis (MSFA) model (De Vito et al., 2019), which is able to identify common and study-specific characteristics in gene expression data across multiple studies.

This approach was also adopted in nutritional epidemiology. For instance, De Vito et al. (2019) analyzed the International Head and Neck Cancer Epidemiology (INHANCE) consortium (Hashibe et al., 2007; Conway et al., 2009) data via MSFA, revealing important common and population-specific diet characteristics and their association with the two cancer types. In this direction, De Vito et al. (2022) adopted a multi-study Bayesian approach in a nutritional epidemiological setting in 4 US field sites (Bronx, Chicago, Miami, San Diego) in the Hispanic Community Health Study/Study of Latinos (HCHS/SOL) (Sorlie et al., 2010). More recently, Stephenson et al. (2020) introduced a generalization of mixture models, namely the Robust Profile Clustering (RPC), to handle diverse populations or studies in a case-control birth defects study in the United States (Yoon et al., 2001). The RPC identifies robust food “global” clusters across all populations and locally population clusters.

All of these approaches highlight the crucial need in nutritional epidemiology to identify common and study diet components concurrently, in order to gain a better understanding of their association with disease outcomes. However, none of these approaches accounts for

covariates or confounders essential to identify the diet signals accurately. Specifically, the diet is affected by numerous confounders (Trichopoulos et al., 1985; Tucker et al., 1997), such as smoking, alcohol, gender, and other covariates, which can obscure both the common and study-specific signals. Thus, not adjusting for multiple potential confounding factors could result in inaccurate conclusions.

In the standard factor analysis framework, models that account for observed covariates are well-studied. For instance, West, 2003 introduced sparse latent factor models with many explanatory variables. This approach enables a more precise assessment of the factor structure, leading to improved breast cancer data predictions. Carvalho et al., 2008 developed a factor regression model that estimated both factor loadings and regression coefficients. This paper provided a modeling approach that improved the characterization of the factor loading patterns in cancer genomic applications by accounting for observed covariates. This approach also showed an increased predictive ability when considering observed covariates. More recently, Avalos-Pacheco et al., 2022 introduced the Bayesian factor regression model, a novel approach that jointly analyzes multiple studies and adjusts for systematic biases, such as batch effects, in a latent factor regression framework. The authors illustrated their analysis' power in both signal detection and predictive ability and empirically showed that inaccurate conclusions can be drawn if batch effects are not appropriately considered.

Although all these methods revealed the crucial need to account for both latent structures and observed variables, none of these methods considered study-specific latent patterns that contribute significantly to the variations of each population. Indeed, these populations or background dietary patterns can reveal essential differences among groups and sometimes mask the shared signal among groups, drastically biasing the associations with the disease. Therefore, it is critical to identify both the shared and study-specific latent components while accounting for other observed covariates, like counfounders and/or

batch effects. To address this challenge, we propose a new modeling approach, the Multi-Study Factor Regression (MSFR) model, which is able to analyze multiple studies/ populations/groups jointly and estimate three different components: (1) the reproducible and shared latent components, (2) the study-specific latent component for each population, (3) the regression coefficients, which are key to detect confounders.

Our work focuses on the Hispanic Community Health Study/Study of Latinos (HCHS/SOL) (National Heart, Lung, and Blood Institute and others, 2009), which is a multi-center epidemiologic study in Hispanic/Latino populations. The HCHS/SOL aims to detect crucial factors impacting the health of Hispanics/Latinos (Sorlie et al., 2010). One of the study’s primary goal is to determine how diet can impact cardiovascular disease (Daviglus et al., 2014) in different Hispanic/Latino origins, specifically in the Cuban, Puerto Rican, Dominican, Mexican, and Central/South American backgrounds. Our MSFR model aims to identify the reproducible dietary components among the different Hispanic/Latino backgrounds and background dietary components while accounting for confounders (i.e., smoking, alcohol, etc.) that can obscure the two dietary signals. In this way, we can assess a more accurate association between dietary patterns and cardiovascular diseases, such as obesity.

The plan of the paper is as follows. Section 2 motivates our new approach by describing the Hispanic Community Health Study/Study of Latinos (HCHS/SOL) and all the variables considered in our analysis. Section 3 presents the multi-study regression approach, including the model definition and model estimation. Section 4 presents the performance of our MSFR in different simulation settings, comparing it with the multi-study factor model, the factor regression model and a two-step approach aimed to correct for covariate effects. Section 5 includes the application of MSFR in the HCHS/SOL study, which motivated our novel method. Section 6 includes the discussion.

2 The Hispanic Community Health Study / Study of Latinos

2.1 The study

The Hispanic Community Health Study/Study of Latinos (HCHS/SOL) is the largest multi-site cohort study of Hispanics/Latinos in the United States. The aim of the study is to provide previously unavailable information on the health status and disease burden of US Hispanics/Latinos and to explore the associations between risk factors and disease incidence during the follow-up. In this manuscript, we consider food and diet as a potential risk for health index, particularly the healthy eating index and cardiovascular disease. The study collected 16,415 adults aged 18-74 years residing in four different sites (Bronx, Chicago, Miami, San Diego) from seven Hispanic/Latino ethnic backgrounds (Cuban, Dominican Republic, Mexican, Puerto Rican, Central, South American, and others). The information is collected at baseline (2008-2011) using a stratified 2-stage probability sampling design, described in detail by LaVange et al. (2010).

The cohort study collects data via two 24-hour recalls, conducted in person at the baseline and via telephone, ≤ 30 days from baseline in the participant's preferred language (English 20% and Spanish 80% of the participants) by trained interviewers. The data is obtained after the two recalls, and based on thousands of common and Hispanic/Latino foods, contains a total of 139 nutrients, nutrient ratios, food-group serving counts, and other food components. All participants (99%) provided at least one recall.

2.2 Selection of subjects and data preprocessing

A total of 14,002 participants' data were collected. We excluded participants who self-identified as belonging to other ethnic backgrounds and/or present recall data unreliable (i.e., vitamin E < 0) and/or show inconsistent (i.e., $< 1st$ or $> 99th$ percentiles) estimates of energy intake. We also removed individuals with missing ethnic background information. After applying all of the above-mentioned exclusion criteria, we performed our analyses on a total of 12,977 participants.

Following De Vito et al. (2022), we selected 53 nutrients that best represent the overall diet for Hispanics/Latinos. We expanded the fat profile for better identifying cardiovascular-disease-related dietary habits (Islam et al., 2019; Lichtenstein, 2003). In particular, we constructed four variables: 1- SCSFA short-chain saturated fatty acids (i.e., butyric acid), 2- MCSFA medium-chain saturated fatty acids (i.e., the sum of caproic acid, caprylic acid, capric acid, and lauric acid), 3- LCSFA long-chain saturated fatty acids (i.e., the sum of myristic acid, palmitic acid, margaric acid, stearic acid and arachidic acid), 4- LCSFA long-chain monounsaturated fatty acids (i.e., the sum of myristoleic acid, palmitoleic acid, oleic acid, and gadoleic acid).

We then derived nutrient intakes from the mean of two available reliable recalls for including all the diet information. We log-transformed the nutrient intakes and standardized the data.

An overview of socio-demographic characteristics for each hispanic background group is provided in Table 1. Note that we only report socio-demographic characteristics included in our model (Section 5).

Hispanic/Latino backgrounds were not equally distributed at each study site. Specifically, the population with Mexican (South American) background is the largest (smaller) among the groups. The majority of individuals were female, never alcohol use, smoking

	Dominican (<i>n</i> = 1257)	Central American (<i>n</i> = 1443)	Cuban (<i>n</i> = 2126)	Mexican (<i>n</i> = 4940)	Puerto Rican (<i>n</i> = 2314)	South American (<i>n</i> = 897)
Gender						
Female	817	862	1139	3031	1350	530
Male	440	583	987	1909	964	367
Education						
< High School	538	595	486	2147	903	212
= High School	249	332	627	1300	609	232
> High School	470	518	1013	1493	802	453
Alcohol Use						
Never	619	858	1159	2521	1226	461
Former	575	521	843	2164	952	410
Current	63	66	124	255	136	26
Cigarette						
0 years	947	999	1077	3241	1122	588
> 0 and < 10 years	170	294	334	1240	541	196
10+ years	140	152	715	459	651	113
BMI* mean(sd)	29.4(5.7)	29.7(5.6)	29.2(5.7)	29.8(5.7)	30.9(6.7)	28.7 (5.2)

Table 1: *Social and Demographic characteristic of the HCHS/SOL consortium for each hispanic background.*

* *Body Mass Index (kg/m²)*

no cigarettes. The category of Education most concentrated was “less than high school”, except for the Cuban background with a concentration on “greater than high school”.

We consider a total of 53 food variables and 5 confounders to best identify the common signals across the 6 different ethnic background groups and the study-specific components for each of these groups.

3 Multi-study factor regression model

We jointly model the data from S different groups, populations, or studies that observe the same p responses. We consider vectors $\mathbf{x}_{is} \in \mathbb{R}^p$, observed for $i = 1, \dots, n$ individuals in $s = 1, \dots, S$ studies. Our method generalizes the traditional multi-study factor analysis (MSFA) (De Vito et al., 2021).

Traditional MSFA models \mathbf{x}_{is} as a linear combination of low-dimensional common factors $\mathbf{f}_{is} \in \mathbb{R}^q$, and group-specific factors $\mathbf{l}_{is} \in \mathbb{R}^{q_s}$, $q + q_s \ll p$:

$$\mathbf{x}_{is} = \mathbf{\Phi}\mathbf{f}_{is} + \mathbf{\Lambda}_s\mathbf{l}_{is} + \mathbf{e}_{is}, \quad (1)$$

where $\mathbf{\Lambda}_s \in \mathbb{R}^{p \times p_s}$ for $s = 1, \dots, S$, is the specific loadings matrix, $\mathbf{\Phi} \in \mathbb{R}^{p \times q}$ is the factor loadings matrix, and $\mathbf{e}_{is} \in \mathbb{R}^p$ is the error, distributed as $\mathbf{e}_{is} \sim N(0, \mathbf{\Psi}_s)$, $s = 1, \dots, S$ where $\mathbf{\Psi}_s = \text{diag}\{\psi_{js}\}_{j=1}^p$ is the idiosyncratic precision matrix of study s . Common and study-specific factors are assumed to be standard normal and independent between them and the errors. Marginally, observations \mathbf{x}_{is} are normally distributed, centered at zero and with covariance matrix $\mathbf{\Sigma}_s = \mathbf{\Phi}\mathbf{\Phi}^\top + \mathbf{\Lambda}_s\mathbf{\Lambda}_s^\top + \mathbf{\Psi}_s$. The covariance matrix allows decomposing the total variance into three distinct parts, i.e. the variance of the common factors $\mathbf{\Phi}\mathbf{\Phi}^\top$, of the study-specific factors $\mathbf{\Lambda}_s\mathbf{\Lambda}_s^\top$ and the error $\mathbf{\Psi}_s$.

Model (1) assumes that the data is explained by unobserved latent factors only, without taking into account prespecified variables that can affect the outcome in practice. For

instance, in our HCHS/SOL application, the MSFA ignores the effect that observed covariates, such as BMI, alcohol and cigarette use, can have on cardiovascular-disease-related dietary habits. In other words, MSFA models the data without allowing for other additional regression effects that do not affect the underlying dietary patterns given in the common and study-specific factors. We will later describe how much inference can suffer when not incorporating such covariate adjustments (Tables 2 and 3, Figures S1, S2, S3, and S4, Supplementary Materials). We tackle this issue by extending Model (1) to incorporate covariate adjustments by adopting a factor regression approach (Avalos-Pacheco et al., 2022; Avalos-Pacheco, 2018; Carvalho et al., 2008). Let \mathbf{b}_{is} be p_b -dimensional vector of known covariates. The Multy-study Factor Regression model is:

$$\mathbf{x}_{is} = \boldsymbol{\beta}\mathbf{b}_{is} + \boldsymbol{\Phi}\mathbf{f}_{is} + \boldsymbol{\Lambda}_s\mathbf{l}_{is} + \mathbf{e}_{is} \quad (2)$$

where $\boldsymbol{\beta} \in \mathbb{R}^{p \times p_b}$ is the matrix of regression coefficients.

We remark that the utility of this model goes beyond our Hispanic Community Health Study. For instance, this model can easily adjust for several covariate effects, such as complex batch effects, by simply setting $\mathbf{b}_{is} \in [0, 1]^S$ as a study indicator. In this setting, $\boldsymbol{\beta}$ captures the mean batch effect adjustment and $\boldsymbol{\Psi}_s$ the variance adjustment.

Maximum likelihood estimation by ECM algorithm

We fit Model (2) using a deterministic Expectation/Conditional Maximization (ECM) optimization (Meng and Rubin, 1993), along the lines of De Vito et al. (2019) to estimate the parameters $\boldsymbol{\theta} = \{\boldsymbol{\Phi}, \boldsymbol{\Lambda}_s, \boldsymbol{\Psi}_s, \boldsymbol{\beta}\}$. Our proposed ECM, summarized in Algorithm 1, maximises the expected complete-data log-likelihood $l_c(\boldsymbol{\theta}) = E_{\mathbf{F}, \mathbf{L}_s | \boldsymbol{\theta}, \mathbf{X}}[p(\boldsymbol{\theta} | \mathbf{F}, \mathbf{L}_s, \mathbf{X})]$ iteratively. For simplicity, let $\tilde{\mathbf{x}}_{is} = \mathbf{x}_{is} - \boldsymbol{\beta}\mathbf{b}_{is}$, and $\hat{\boldsymbol{\theta}} = \{\hat{\boldsymbol{\Phi}}, \hat{\boldsymbol{\Lambda}}_s, \hat{\boldsymbol{\Psi}}_s, \hat{\boldsymbol{\beta}}\}$ be the current value of the estimated parameters.

Algorithm 1: ECM algorithm for Multi-study Factor Regression

initialize $\widehat{\Phi} = \Phi^{(0)}, \widehat{\Lambda}_s = \Lambda_s^{(0)}, \widehat{\Psi}_s = \Psi_s^{(0)}, \widehat{\beta} = \beta^{(0)}$

while $t < T$ and $\epsilon > \epsilon^*$ do

E-step[§]:

$$\begin{aligned} E[\mathbf{f}_{is} | \widetilde{\mathbf{x}}_{is}, \widehat{\theta}] &= \mathbf{E}_{f_i} = \delta \widetilde{\mathbf{x}}_{is}, & E[l_{is} | \widetilde{\mathbf{x}}_{is}, \widehat{\theta}] &= \mathbf{E}_{l_{is}} = \delta_s \widetilde{\mathbf{x}}_{is}, \\ E[\mathbf{C}_{\widetilde{\mathbf{x}}_s \widetilde{\mathbf{x}}_s} | \widetilde{\mathbf{x}}_{is}, \widehat{\theta}] &= \mathbf{E}_{\widetilde{\mathbf{x}}_s \widetilde{\mathbf{x}}_s} = \mathbf{C}_{\widetilde{\mathbf{x}}_s \widetilde{\mathbf{x}}_s}, & E[\mathbf{C}_{\widetilde{\mathbf{x}}_s l_s} | \widetilde{\mathbf{x}}_{is}, \widehat{\theta}] &= \mathbf{E}_{\widetilde{\mathbf{x}}_s l_s} = \mathbf{C}_{\widetilde{\mathbf{x}}_s l_s} \delta_s^\top, \\ E[\mathbf{C}_{\widetilde{\mathbf{x}}_s f} | \widetilde{\mathbf{x}}_{is}, \widehat{\theta}] &= \mathbf{E}_{\widetilde{\mathbf{x}}_s f} = \mathbf{C}_{\widetilde{\mathbf{x}}_s \widetilde{\mathbf{x}}_s} \delta_s^\top, & E[\mathbf{C}_{ff} | \widetilde{\mathbf{x}}_{is}, \widehat{\theta}] &= \mathbf{E}_{ff} = \delta \mathbf{C}_{\widetilde{\mathbf{x}}_s \widetilde{\mathbf{x}}_s} \delta_s^\top + \Delta, \\ E[\mathbf{C}_{l_s l_s} | \widetilde{\mathbf{x}}_{is}, \widehat{\theta}] &= \mathbf{E}_{l_s l_s} = \delta_s \mathbf{C}_{\widetilde{\mathbf{x}}_s \widetilde{\mathbf{x}}_s} \delta_s^\top + \Delta_s & E[\mathbf{C}_{fl_s} | \widetilde{\mathbf{x}}_{is}, \widehat{\theta}] &= \mathbf{E}_{fl_s} = \delta \mathbf{C}_{\widetilde{\mathbf{x}}_s \widetilde{\mathbf{x}}_s} \delta_s^\top + \Delta_{fl}. \end{aligned}$$

CM-step:

$$\begin{aligned} \widehat{\Psi}_s &= \text{diag} \left\{ \mathbf{E}_{\widetilde{\mathbf{x}}_s \widetilde{\mathbf{x}}_s} + \widehat{\Phi} \mathbf{E}_{ff} \widehat{\Phi}^\top + \widehat{\Lambda}_s \mathbf{E}_{l_s l_s} \widehat{\Lambda}_s^\top - 2 \mathbf{E}_{\widetilde{\mathbf{x}}_s f} \widehat{\Phi}^\top - 2 \mathbf{E}_{\widetilde{\mathbf{x}}_s l_s} \widehat{\Lambda}_s^\top + 2 \widehat{\Phi} \mathbf{E}_{fl_s} \widehat{\Lambda}_s^\top \right\} \\ \text{vec}(\widehat{\Phi}) &= \sum_{s=1}^S \left(\mathbf{E}_{ff}^\top \otimes n_s \widehat{\Psi}_s^{-1} \right) \text{vec} \left(n_s \widehat{\Psi}_s^{-1} \mathbf{E}_{\widetilde{\mathbf{x}}_s f} - n_s \widehat{\Psi}_s^{-1} \widehat{\Lambda}_s \mathbf{E}_{fl_s}^\top \right) \\ \widehat{\Lambda}_s &= \left(\mathbf{E}_{x_s f} - \widehat{\Phi} \mathbf{E}_{fl_s} \right) \left(\mathbf{E}_{l_s l_s} \right)^{-1} \\ \widehat{\beta} &= \left[\sum_{s=1}^S \sum_i^{n_s} (\mathbf{x}_{is} - \widehat{\Phi} \mathbf{E}_{f_i} - \widehat{\Lambda}_s \mathbf{E}_{l_{is}}) \mathbf{b}_{is}^\top \right] \left[\sum_{s=1}^S \sum_i^{n_s} (\mathbf{b}_{is} \mathbf{b}_{is}^\top) \right]^{-1} \end{aligned}$$

set $\theta^{(t+1)} = \widehat{\theta}$

compute $t = t + 1$ and $\epsilon = |l^{(t+1)} - l^{(t)}|$, with $l^{(t+1)} = l_c(\theta^{(t)}) + \frac{l_c(\theta^{(t+1)}) - l_c(\theta^{(t)})}{1 - c^{(t)}}$, and

$$c^{(t)} = \frac{l_c(\theta^{(t+1)}) - l_c(\theta^{(t)})}{l_c(\theta^{(t)}) - l_c(\theta^{(t-1)})}$$

end

[§] where

$$\begin{aligned} \mathbf{C}_{\widetilde{\mathbf{x}}_s \widetilde{\mathbf{x}}_s} &= \frac{\sum_{i=1}^{n_s} \widetilde{\mathbf{x}}_{is} \widetilde{\mathbf{x}}_{is}^\top}{n_s}, & \mathbf{C}_{ff} &= \frac{\sum_{i=1}^{n_s} \mathbf{f}_{is} \mathbf{f}_{is}^\top}{n_s}, & \mathbf{C}_{l_s l_s} &= \frac{\sum_{i=1}^{n_s} l_{is} l_{is}^\top}{n_s}, \\ \mathbf{C}_{\widetilde{\mathbf{x}}_s f} &= \frac{\sum_{i=1}^{n_s} \widetilde{\mathbf{x}}_{is} \mathbf{f}_{is}^\top}{n_s}, & \mathbf{C}_{\widetilde{\mathbf{x}}_s l_s} &= \frac{\sum_{i=1}^{n_s} \widetilde{\mathbf{x}}_{is} l_{is}^\top}{n_s}, & \mathbf{C}_{fl_s} &= \frac{\sum_{i=1}^{n_s} \mathbf{f}_{is} l_{is}^\top}{n_s}, \end{aligned}$$

$$\Delta_{fl} = \text{Cov}[l_{is}, \mathbf{f}_{is} | \widetilde{\mathbf{x}}_{is}, \theta_{t-1}] = \Phi^\top \Sigma_s^{-1} \Lambda_s,$$

and

$$\begin{aligned} \delta &= \Phi^\top \Sigma_s^{-1}, & \Delta &= \text{Var}[\mathbf{f}_{is} | \widetilde{\mathbf{x}}_{is}, \theta_{t-1}] = \mathbf{I}_q - \Phi^\top \Sigma_s^{-1} \Phi, \\ \delta_s &= \Lambda_s^\top \Sigma_s^{-1}, & \Delta_s &= \text{Var}[l_{is} | \widetilde{\mathbf{x}}_{is}, \theta_{t-1}] = \mathbf{I}_{q_s} - \Lambda_s^\top \Sigma_s^{-1} \Lambda_s. \end{aligned}$$

In the E-step, we obtained the expected complete-data log-likelihood

$$\begin{aligned} l_c(\theta) &= \sum_{s=1}^S \left\{ -\frac{n_s}{2} \log |\Psi_s| - \frac{n_s}{2} \text{tr} \left[\Psi_s^{-1} \frac{\sum_i^{n_s} \left(E[\widetilde{\mathbf{x}}_{is} \widetilde{\mathbf{x}}_{is}^\top | \widetilde{\mathbf{x}}_{is}, \widehat{\theta}] \right)}{n_s} \right. \right. \\ &\quad \left. \left. + \Phi E[\mathbf{f}_{is} \mathbf{f}_{is}^\top | \widetilde{\mathbf{x}}_{is}, \widehat{\theta}] \Phi^\top + \Lambda_s E[l_{is} l_{is}^\top | \widetilde{\mathbf{x}}_{is}, \widehat{\theta}] \Lambda_s^\top - 2 E[\widetilde{\mathbf{x}}_{is} \mathbf{f}_{is}^\top | \widetilde{\mathbf{x}}_{is}, \widehat{\theta}] \Phi^\top \right. \right. \\ &\quad \left. \left. - 2 E[\widetilde{\mathbf{x}}_{is} l_{is}^\top | \widetilde{\mathbf{x}}_{is}, \widehat{\theta}] \Lambda_s^\top + 2 \Phi E[\mathbf{f}_{is} l_{is}^\top | \widetilde{\mathbf{x}}_{is}, \widehat{\theta}] \Lambda_s^\top \right] \right\} + C, \end{aligned} \quad (3)$$

where C is a constant. Equation (3) depends on the latent factors \mathbf{f}_{is} and \mathbf{l}_{is} in terms of their conditional mean and their conditional second moments, shown in Algorithm 1 and Supplement A. All the moments are computed based on the multivariate normal distribution.

Note that the conditional expectations require to invert the $p \times p$ covariate matrix $\widehat{\Sigma}_s$, through

$$\boldsymbol{\delta} = \widehat{\Phi}^\top \widehat{\Sigma}_s^{-1}, \quad \boldsymbol{\delta}_s = \widehat{\Lambda}_s^\top \widehat{\Sigma}_s^{-1}, \quad (4)$$

which can be cumbersome and challenging as the number of the variables p increases. To address this issue, we apply the Woodbury matrix identity (Morgenstern and Woodbury, 1950) twice, obtaining

$$\boldsymbol{\delta} = (\mathbf{I}_q + \widehat{\Phi}^\top \widehat{\mathbf{W}}_{\Lambda_s} \widehat{\Phi})^{-1} \widehat{\Phi}^\top \widehat{\mathbf{W}}_{\Lambda_s}, \quad \boldsymbol{\delta}_s = (\mathbf{I}_{q_s} + \widehat{\Lambda}_s^\top \widehat{\mathbf{W}}_{\Phi} \widehat{\Lambda}_s)^{-1} \widehat{\Lambda}_s^\top \widehat{\mathbf{W}}_{\Phi}, \quad (5)$$

with

$$\begin{aligned} \widehat{\mathbf{W}}_{\Lambda_s} &= (\widehat{\Lambda}_s \widehat{\Lambda}_s^\top + \widehat{\Psi}_s)^{-1} = \widehat{\Psi}_s^{-1} - \widehat{\Psi}_s^{-1} \widehat{\Lambda}_s (\mathbf{I}_{q_s} + \widehat{\Lambda}_s^\top \widehat{\Psi}_s^{-1} \widehat{\Lambda}_s)^{-1} \widehat{\Lambda}_s^\top \widehat{\Psi}_s^{-1} \\ \widehat{\mathbf{W}}_{\Phi} &= (\widehat{\Phi} \widehat{\Phi}^\top + \widehat{\Psi}_s)^{-1} = \widehat{\Psi}_s^{-1} - \widehat{\Psi}_s^{-1} \widehat{\Phi} (\mathbf{I}_q + \widehat{\Phi}^\top \widehat{\Psi}_s^{-1} \widehat{\Phi})^{-1} \widehat{\Phi}^\top \widehat{\Psi}_s^{-1}. \end{aligned} \quad (6)$$

We have carried the inference of $\mathbf{E}_{f_{is}}$ and $\mathbf{E}_{l_{is}}$ using Equation (6).

In the CM-step, we maximize $l_c(\boldsymbol{\theta})$ with respect to $\Phi, \Lambda_s, \Psi_s, \beta$. For simplicity, we can re-write Equation (3) as

$$\begin{aligned} l_c(\boldsymbol{\theta}) &= \sum_{s=1}^S \left(-\frac{n_s}{2} \log |\Psi_s| - \frac{n_s}{2} \text{tr} \left[\Psi_s^{-1} (\mathbf{E}_{\tilde{x}_s \tilde{x}_s} + \Phi \mathbf{E}_{f_s f_s} \Phi^\top \right. \right. \\ &\quad \left. \left. + \Lambda_s \mathbf{E}_{l_s l_s} \Lambda_s^\top - 2 \mathbf{E}_{\tilde{x}_s f_s} \Phi^\top - 2 \mathbf{E}_{\tilde{x}_s l_s} \Lambda_s^\top + 2 \Phi \mathbf{E}_{f_s l_s} \Lambda_s^\top) \right] \right), \end{aligned} \quad (7)$$

with $\mathbf{E}_{\tilde{x}_s \tilde{x}_s}, \mathbf{E}_{f_s f_s}, \mathbf{E}_{l_s l_s}, \mathbf{E}_{\tilde{x}_s f_s}$ and $\mathbf{E}_{f_s l_s}$ as in Algorithm 1. We obtain the updates for each parameter setting the partial derivatives of $l_c(\boldsymbol{\theta})$ to zero, and update each of them iteratively while keeping the others fixed at their most recent update. The updates for the precision

Ψ_s , common Φ , and study-specific loadings matrices Λ_s are obtained analogously to the ECM updates in the MSFA (De Vito et al., 2019), with $\tilde{\mathbf{x}}_{is} = \mathbf{x}_{is} - \beta \mathbf{b}_{is}$, maximizing Equation (7) w.r.t. Φ, Λ_s, Ψ_s :

$$\begin{aligned} \hat{\Psi}_s &= \text{diag} \left\{ \mathbf{E}_{\tilde{x}_s \tilde{x}_s} + \hat{\Phi} \mathbf{E}_{ff} \hat{\Phi}^\top + \hat{\Lambda}_s \mathbf{E}_{l_s l_s} \hat{\Lambda}_s^\top - 2 \mathbf{E}_{\tilde{x}_s f} \hat{\Phi}^\top - 2 \mathbf{E}_{\tilde{x}_s l_s} \hat{\Lambda}_s^\top + 2 \hat{\Phi} \mathbf{E}_{fl_s} \hat{\Lambda}_s^\top \right\} \\ \text{vec}(\hat{\Phi}) &= \sum_{s=1}^S \left(\mathbf{E}_{ff}^\top \otimes n_s \hat{\Psi}_s^{-1} \right) \text{vec} \left(n_s \hat{\Psi}_s^{-1} \mathbf{E}_{\tilde{x}_s f} - n_s \hat{\Psi}_s^{-1} \hat{\Lambda}_s \mathbf{E}_{fl_s}^\top \right) \\ \hat{\Lambda}_s &= \left(\mathbf{E}_{x_s f} - \hat{\Phi} \mathbf{E}_{fl_s} \right) \left(\mathbf{E}_{l_s l_s} \right)^{-1}, \end{aligned} \quad (8)$$

where \otimes is the Kronecker product, vec is the vec operator, and the linear equation is solved with the Lyapunov Equation. More details about the optimizations can be found in Supplementary A.

To estimate the coefficients β , we first expand Equation (3):

$$l_c(\boldsymbol{\theta}) \propto \sum_{s=1}^S \left\{ -\frac{n_s}{2} \text{tr} \left[\frac{\Psi_s^{-1} \sum_i^{n_s} \left(-2 \mathbf{x}_{is} \mathbf{b}_{is}^\top \beta^\top + \beta \mathbf{b}_{is} \mathbf{b}_{is}^\top \beta^\top + 2 \beta \mathbf{b}_{is} \mathbf{E}_{f_i}^\top \Phi^\top + 2 \beta \mathbf{b}_{is} \mathbf{E}_{l_{is}}^\top \Lambda_s^\top \right)}{n_s} \right] \right\}. \quad (9)$$

We then take the derivative and the expected values of Equation (9)

$$\frac{\partial l_c(\boldsymbol{\theta})}{\partial \beta} = \sum_{s=1}^S \left(-\frac{n_s}{2} \Psi_s^{-1} \left[\frac{\sum_i^{n_s} 2 \left(\beta \mathbf{b}_{is} \mathbf{b}_{is}^\top - (\mathbf{x}_{is} - \Phi \mathbf{E}_{f_i} - \Lambda_s \mathbf{E}_{l_{is}}) \mathbf{b}_{is}^\top \right)}{n_s} \right] \right) = 0, \quad (10)$$

and solve Equation (10) to obtain:

$$\hat{\beta} = \left[\sum_{s=1}^S \sum_i^{n_s} (\mathbf{x}_{is} - \hat{\Phi} \mathbf{E}_{f_i} - \hat{\Lambda}_s \mathbf{E}_{l_{is}}) \mathbf{b}_{is}^\top \right] \left[\sum_{s=1}^S \sum_i^{n_s} (\mathbf{b}_{is} \mathbf{b}_{is}^\top) \right]^{-1}. \quad (11)$$

The stopping criterion used for our proposed ECM algorithm is based on Aitken acceleration (McLachlan, 2008). Algorithm 1 is stopped when a tolerance $\epsilon^* = |l^{(t+1)} - l^{(t)}|$, with

$l^{(t+1)} = l_c(\boldsymbol{\theta}^{(t)}) + \frac{l_c(\boldsymbol{\theta}^{(t+1)}) - l_c(\boldsymbol{\theta}^{(t)})}{1 - c^{(t)}}$, and $c^{(t)} = \frac{l_c(\boldsymbol{\theta}^{(t+1)}) - l_c(\boldsymbol{\theta}^{(t)})}{l_c(\boldsymbol{\theta}^{(t)}) - l_c(\boldsymbol{\theta}^{(t-1)})}$ in the complete log-likelihood change is reached, or a maximum number of iterations T have been completed. By default we set $\epsilon^* = 10^{-7}$ and $T = 50,000$.

The selection of the dimension of the common and study-specific factors q and q_s is made by choosing the model that leads to the best Akaike information criterion (AIC) (Akaike, 1974) or the Bayesian information criterion (BIC) (Schwarz, 1978). More details about the latent cardinality selection will be discussed in Sections §4 and §5.

Initialization of the ECM algorithm

Parameter initialization is crucial to obtain better local modes and reduce computational time, as the ECM algorithm can be sensitive to parameter initialization. Here, we propose a simple two-step least-squares initialisation by stacking all the S study-data in a single data set $\mathbf{X}^\top \in \mathbb{R}^{n \times p}$, $n = n_1 + \dots + n_S$:

Step 1 initialize $\boldsymbol{\beta}^{(0)} = [\mathbf{B}\mathbf{B}^\top]^{-1} \mathbf{B}\mathbf{X}^\top$ with $\mathbf{X}^\top \in \mathbb{R}^{n \times p}$, $\mathbf{B}^\top \in \mathbb{R}^{n \times p_b}$

Step 2 let $\tilde{\mathbf{X}} = \mathbf{X} - \boldsymbol{\beta}^{(0)}\mathbf{B}$. Initialize the extra parameters as the Multi-study factor analysis:

1. perform a Principal Components Analysis (PCA) on $\tilde{\mathbf{X}}$ and initialize $\boldsymbol{\Phi}^{(0)}$ with the first q principal components, and
2. perform factor analysis for each $\tilde{\mathbf{X}}_s$, $s = 1, \dots, S$, and initialize $\boldsymbol{\Lambda}^{(0)}$ and $\boldsymbol{\Psi}^{(0)}$ with the obtained loading matrices and unharnesses, respectively.

Identifiability Considerations

The MSFR model, like other standard factor analysis models, is non-identifiable up orthogonal transformations of the loadings (common $\boldsymbol{\Phi}$ and study specific $\boldsymbol{\Lambda}_s$) and loadings

sign switch. In addition to those sources of non-identification, the MSFR model has an indeterminacy of the covariance Σ_s decomposition.

The rotation identifiability arises since any orthogonal transformation of the factors and the loading matrices, common and study-specific, lead to the same distribution of \mathbf{x}_{is} . Thus, the marginal distribution of \mathbf{x}_{is} can equivalently be redefined as a multivariate normal with covariance matrix $\Sigma_s = \tilde{\Phi}\tilde{\Phi}^\top + \tilde{\Lambda}_s\tilde{\Lambda}_s^\top + \Psi_s$, where $\tilde{\Phi} = \Phi\mathbf{R}$ and $\tilde{\Lambda}_s = \Lambda_s\mathbf{R}_s$, with $\mathbf{R} \in \mathbb{R}^{q \times q}$ and $\mathbf{R}_s \in \mathbb{R}^{q_s \times q_s}$ orthogonal matrices. Furthermore, Model (2) can be rewritten as $\mathbf{x}_{is} = \beta\mathbf{b}_{is} + \tilde{\Phi}\tilde{\mathbf{f}}_{is} + \tilde{\Lambda}_s\tilde{\mathbf{l}}_{is} + \mathbf{e}_{is}$, with $\tilde{\mathbf{f}}_{is} = \mathbf{R}^\top \mathbf{f}_{is}$ and $\tilde{\mathbf{l}}_{is} = \mathbf{R}_s^\top \mathbf{l}_{is}$. In the factor analysis literature, several strategies have been developed to tackle this issue, such as performing a varimax rotation (Kaiser, 1958), or restricting the loading matrix to be lower triangular (Lopes and West, 2004; Carvalho et al., 2008) or generalized lower triangular (Frühwirth-Schnatter et al., 2023). Here, we extend the traditional varimax rotation to both the Φ and Λ_s . Such alternative was selected due to its interpretability. MSFR is also not uniquely identified due to sign switching of the loading matrices Φ and Λ_s . We fix this mild issue by constraining the sign of a subset of loadings.

Under varimax rotation and sign constraints, a full rank loading matrix is uniquely determined in regular factor analysis, giving the error term. However, in multi-study latent models, an additional source of non-identifiability arises, the indeterminacy of the covariance Σ_s decomposition. More in detail, the difference between the covariance matrix and the idiosyncratic precisions can be redefined as $\Sigma_s - \Psi_s = \Phi^*\Phi^{*\top} + \Lambda_s^*\Lambda_s^{*\top}$, from where column vectors of Φ and Λ_s can move from one loading matrix to the other. To solve this issue, we follow the strategy of (De Vito et al., 2019), and constraint the $[\Phi, \Lambda_1, \dots, \Lambda_S] \in \mathbb{R}^{p \times (q + \sum_{s=1}^S q_s)}$ matrix, containing both the common and study specific loadings, to have a full column rank $q + \sum_{s=1}^S q_s \leq p$. Thus, the span of the column vectors of $\Sigma_s - \Psi_s$ is equal to the sum of the span of the column vectors of Φ and Λ_s , leading to uniquely determined

loading matrices.

4 Simulation Study

We first use simulation studies to assess the ability of our MSFR model to detect the true signals for both the common and the study-specific and outperform the standard MSFA in the presence of observed covariates. Specifically, we compare the MSFR with MSFA to illustrate how much inference can suffer when not accounting for covariate effects. To evaluate if the covariate effect can be removed from the data and then adopt the MSFA to the residuals, we fit a linear regression (LR) model, followed by MSFA estimation on the residuals, here called (MSFA&LR). Moreover, we compare the MSFR with the vanilla Factor Regression (FR) (Avalos-Pacheco et al., 2022; Carvalho et al., 2008) to assess the advantages of estimating the study-specific factors. The R-code for our methods is available at <https://github.com/rdevito/MSFR>.

We consider various scenarios with different sample sizes n_s , number of studies S , number of observed variables p , structure of β , and structure of Σ , as shown in Table 2. Scenario 1 shows the advantages of our method in situations with small covariate effects. Scenarios 2 and 3 closely mimic the case study data, the HCHS/SOL dataset, with its same number of studies and patient characteristics varying only in the structure of β , changing the dimension of p_b . For all the scenarios, we simulated 100 collections of datasets from $N(\beta \mathbf{b}_{i_s}, \Sigma_s)$, with $\Sigma_s = (\Phi \Phi^\top + \Lambda_s \Lambda_s^\top + \Psi_s)$. The common Φ and study specific Λ_s loading matrices are assumed to be sparse, with one-third of non-zero entries, randomly generated from the uniform densities $\Phi \sim \text{sign} \times U(0.6, 1)$, with $\text{sign} \sim U\{-1, 1\}$ and $\Lambda_s \sim U(-1, 1)$. Finally, the idiosyncratic precision matrices, Ψ_s , were assumed to be diagonal matrices with the entries generated uniformly between (0,1).

Table 2 shows the mean results across 100 simulations of (i) the selected number of common and study-specific factors, \hat{q} and \hat{q}_s respectively, and (ii) the RV coefficient (Robert and Escoufier, 1976) between the ground truth and the reconstructed value for the coefficients $\hat{\beta}$, the common $\hat{\Phi}$ and the study-specific loadings $\hat{\lambda}_s$, and the total covariance $\hat{\Sigma}_s$ for all the studies. The RV coefficient $\in [0, 1]$ is a multivariate generalization of the squared Pearson correlation coefficient. The higher the value of the RV coefficient, the better the reconstruction. For each simulation, we considered a grid of possible values for \hat{q} and \hat{q}_s , and we fit the models for all the grid values and performed model selection. Table 2 displays the results for the selected models following the Akaike information criterion (AIC) (Akaike, 1974) and the Bayesian information criterion (BIC) (Schwarz, 1978) approaches for the three different scenarios.

The results showed the advantages of using our proposed method. MSFR presented the highest RV for the common and study-specific loading matrices as well as for the whole covariances. We can also see that MSFR estimated \hat{q} and \hat{q}_s accurately in all the scenarios, independently of the model selection criteria (BIC and AIC), showing a most robust behaviour than MSFA&LR and MSFA. As expected, FR required a higher number of factors to take into account the impact of the study-specific factors. Likewise, MSFA required more factors since it does not consider the covariate effects. MSFA&LR outperformed all the methods in the reconstruction of β , but showed the worst performance in the reconstruction of \hat{q} , \hat{q}_s , Λ_s and Φ in all the scenarios, highlighting the limitations of using two-step procedures relative to a joint estimation of the multiple-factor model and covariate effects. We then assess the reconstructions of β , Σ_{Φ} , λ_s and Σ_s obtained with the AIC criteria for all the methods and scenarios.

Table 2: Average RV over 100 simulations

		\hat{q}	\hat{q}_s	$\hat{\beta}$	$\hat{\Phi}$	$\hat{\lambda}_1$	$\hat{\lambda}_2$	$\hat{\lambda}_3$	$\hat{\lambda}_4$	$\hat{\lambda}_5$	$\hat{\lambda}_6$	$\hat{\Sigma}_1$	$\hat{\Sigma}_2$	$\hat{\Sigma}_3$	$\hat{\Sigma}_4$	$\hat{\Sigma}_5$	$\hat{\Sigma}_6$	
Scenario 1: $q = 3, q_s = 1, S = 2, p_b = 2, p = 20, n_s = \{500, 500, 500\}$																		
BIC	MSFR	3.00	1.00	0.978	0.996	0.959	0.931					0.974	0.987					
	MSFA&LR	3.00	1.00	0.993	0.973	0.922	0.875					0.923	0.942					
	MSFA	4.95	1.04	NA	0.915	0.900	0.844					0.889	0.904					
	FR	3.57	NA	0.991	0.956	NA	NA					0.912	0.888					
AIC	MSFR	3.14	1.19	0.978	0.994	0.936	0.904					0.972	0.986					
	MSFA&LR	1.51	3.20	0.993	0.626	0.365	0.178					0.585	0.608					
	MSFA	2.80	3.94	NA	0.759	0.399	0.188					0.719	0.736					
	FR	3.84	NA	0.991	0.948	NA	NA					0.913	0.885					
Scenario 2: $q = 4, q_s = 1, S = 6, p_b = 7, p = 42, n_s = \{1257, 1444, 2126, 4940, 2314, 897\}$																		
BIC	MSFR	4.00	1.00	0.952	1.000	0.983	0.982	0.990	0.995	0.991	0.981	0.999	0.999	0.999	0.999	0.999	0.999	0.999
	MSFA&LR	1.14	4.13	0.999	0.602	0.017	0.036	0.033	0.002	0.006	0.011	0.841	0.848	0.858	0.866	0.832	0.847	
	MSFA	8.22	2.51	NA	0.953	0.927	0.908	0.939	0.982	0.973	0.927	0.965	0.965	0.964	0.966	0.966	0.966	
	FR	5.00	NA	0.998	0.971	NA	NA	NA	NA	NA	NA	0.860	0.874	0.868	0.872	0.876	0.892	
AIC	MSFR	4.12	1.00	0.952	1.000	0.983	0.982	0.990	0.995	0.991	0.981	0.999	0.999	0.999	0.999	0.999	0.999	
	MSFA&LR	3.00	5.00	0.999	0.815	0.206	0.235	0.222	0.207	0.208	0.218	0.931	0.932	0.937	0.938	0.930	0.932	
	MSFA	8.39	5.00	NA	0.953	0.924	0.907	0.938	0.981	0.971	0.929	0.966	0.966	0.965	0.967	0.966	0.965	
	FR	5.00	NA	0.998	0.971	NA	NA	NA	NA	NA	NA	0.860	0.874	0.868	0.872	0.876	0.892	
Scenario 3: $q = 4, q_s = 1, S = 6, p_b = 9, p = 42, n_s = \{1257, 1444, 2126, 4940, 2314, 897\}$																		
BIC	MSFR	3.99	1.00	0.940	0.999	0.970	0.975	0.982	0.986	0.981	0.971	0.999	0.999	0.999	0.999	0.999	0.999	
	MSFA&LR	1.36	4.17	0.998	0.617	0.033	0.074	0.050	0.022	0.026	0.030	0.852	0.856	0.864	0.869	0.847	0.851	
	MSFA	8.06	2.28	NA	0.923	0.925	0.903	0.936	0.982	0.976	0.920	0.929	0.930	0.929	0.929	0.931	0.928	
	FR	5.00	NA	0.998	0.971	NA	NA	NA	NA	NA	NA	0.859	0.874	0.867	0.871	0.876	0.892	
AIC	MSFR	4.16	1.00	0.940	0.999	0.970	0.975	0.982	0.986	0.981	0.971	0.999	0.999	0.999	0.999	0.999	0.999	
	MSFA&LR	2.60	5.00	0.998	0.787	0.126	0.181	0.136	0.120	0.120	0.135	0.923	0.923	0.929	0.928	0.923	0.922	
	MSFA	9.06	5.00	NA	0.923	0.923	0.898	0.936	0.982	0.975	0.922	0.928	0.929	0.928	0.928	0.930	0.927	
	FR	5.00	NA	0.998	0.971	NA	NA	NA	NA	NA	NA	0.859	0.874	0.867	0.871	0.876	0.892	

Supplementary B Figure S1 displays the heatmaps of the true β and Σ_{Φ} , and their average estimations (left panel), as well as the RV's box-plots for β and Φ (right panel). Figure S2 shows the box-plots of the RV coefficients of λ_s and Σ_s . Overall, MSFR performs better than the other methods, with the smallest variance in all cases, except for β (Figure S1). It is important to highlight that even though MSFA achieved a competitive reconstruction of Φ , the average Σ_{Φ} estimates over the simulations are less precise, as displayed in the heatmaps in Figure S2. Finally, Supplementary C, Figures S3 and S4 present the results of the reconstructions of β , Σ_{Φ} , λ_s and Σ_s obtained via the BIC criterion. The results showed that the performance of our competitors varied significantly, further corroborating that those methods may not be robust to the model selection criteria.

5 The HCHS/SOL application

We demonstrate the usefulness of our method by performing four different analyses on the HCHS/SOL. First, we compare the prediction accuracy between the MSFR and the MSFA to show the power of our method in predictive ability. Second, we explore the common and study-specific factors loadings among the five different background groups of the HCHS/SOL. Third, we associate the common and study-specific loadings with food groups. Fourth, we validate our obtained dietary patterns, both common and study-specific, associating each factor with the alternative eating index(AHEI-2010) - a measure of overall diet quality previously related to cardiometabolic disease risk (Liese et al., 2015).

Predictive analyses. We compare the k-fold cross-validation (setting k=5) prediction errors computed by our MSFR and the MSFA. Thus, we fit both the MSFR and the MSFA model on a random 80% of the data, followed by a different 80% for different folds. We then evaluate the prediction error on the remaining 20% in each fold. Predictions are performed

as

$$\text{MSFR: } \hat{\mathbf{x}}_{is} = \hat{\beta} \hat{\mathbf{b}}_{is} + \hat{\Phi}^{MSFR} \hat{\mathbf{f}}_{is} + \hat{\Lambda}_s^{MSFR} \hat{\mathbf{l}}_{is} \quad \text{MSFA: } \hat{\mathbf{x}}_{is} = \hat{\Phi}^{MSFA} \hat{\mathbf{f}}_{is} + \hat{\Lambda}_s^{MSFA} \hat{\mathbf{l}}_{is},$$

where $\hat{\Phi}^{MSFR}$ is the common factor loadings obtained with the MSFR method, while $\hat{\Phi}^{MSFA}$ is the common factor loadings obtained with the MSFA method; $\hat{\Lambda}_s^{MSFR}$ is specific factor loadings estimated with MSFR, while $\hat{\Lambda}_s^{MSFA}$ is specific factor loadings. The factor scores are then computed using the Bartlett method since scores are uncorrelated between each other (DiStefano et al., 2009), see Supplement D for further details, by using different parameters obtained in the MSFR and MSFA. Thurstone method for estimating factor score lead to similar results. We then assessed the mean squared error (MSE) of prediction for each fold as $MSE = \frac{1}{n} \sum_{s=1}^S \sum_{i=1}^{n_s} (\mathbf{x}_{is} - \hat{\mathbf{x}}_{is})^2$, using the 20% of the samples in each study set aside for each cross-validation iteration. We averaged all the MSE obtained in each fold. Table 3 shows the obtained MSE for the MSFR and the MSFA, obtained with the factor scores computed via Bartlett and Thurstone. The MSE is 4% smaller for MSFR than for MSFA. This analysis reveals how MSFR borrows strength across studies in estimating the factor loadings and clearly detecting factor loading signals by removing all the covariates noise that can impact them. Thus, our predictive power in independent observations is not only preserved but also improved.

Factor loadings analyses.

We considered two main tasks: to analyze the estimated common and study-specific factors loadings, Φ and Λ_s , respectively, and to study the loading association with different food groups.

The MSFR model selected $\hat{q} = 4$ common factors and $\hat{q}_s = 1$ study-specific factor for the six different backgrounds (obtained with the AIC procedure). The common factors explained 62.5% of the total variation, each of which explained 23.8%, 15.5%, 9.8% and

<i>Method</i>	<i>MSE</i>	
	Bartlett	Thurstone
MSFR	1.70	1.62
MSFA	1.76	1.68

Table 3: Mean square error (*MSE*) obtained via *k*-fold cross validation for both the multi-study factor regression model (*MSFR*) and the multi-study factor analysis model (*MSFA*). Factor scores are obtained with the Bartlett and Thurstone method.

6.9% of the total variance. The total variance explained by each study-specific factor range between 6.9% (Dominican, Mexican, and Puerto Rican background) to 6.5% (Cuban background). Thus, no differences are detected among the explained variance for each study-specific loading. We remark that all the factors, common and study-specific, explain more than 5% of the total variance, a trade-off generally considered in factor analysis, confirming our factor dimension estimation.

We proceed by inspecting the factor structures. Figure 1 provides a visual representation of the common and study-specific loadings, on the left and right panels, respectively. In order to facilitate interpretation and thus name each factor, we performed a varimax rotation (Kaiser, 1958) for the common loading matrix. This rotation was unnecessary for Λ_s as our MSFR estimate only one extra study-specific loading.

The varimax rotation in the common loadings maximizes the variance in the squared rotated loadings, making the loadings extreme and positive for a better interpretation. Factor 1, namely Plant-based foods, showed high-valued loadings on vegetable protein, phosphorus, magnesium, iron, zinc, copper, potassium, manganese, thiamin, niacin, pantothenic acid, vitamin B6, natural folate, soluble and insoluble dietary fiber. Factor 2, namely Animal products, displayed high-valued loadings in animal protein, cholesterol, long-chain saturated fatty acids (LCSFA), long-chain monounsaturated fatty acids

(LCMFA), linolenic acid, arachidonic acid, total trans fatty acid, selenium, sodium, and natural alpha-tocopherol. Factor 3, namely Dairy products, exhibited high-valued loadings on short- and medium-chain saturated fatty acids, calcium, riboflavin, retinol, and vitamin D. Factor 4, namely Seafood, presented high-valued loadings on eicosapentaenoic acid (EPA), docosapentaenoic acid (DPA), and docosahexaenoic acid (DHA).

In the absence of any rotation in the specific factor loadings, we based our interpretation on the opposite (positive and negative) signs or colors (blue and dark red, respectively) illustrated in the study-specific factor loading heatmap (Figure 1 right panel). They displayed some similarities, showing a general behavior with positive loadings for the animal food source (i.e., animal proteins, cholesterol, arachidonic acid, vitamin B12, vitamin D) and negative loadings for the vegetable source (i.e., vegetable protein, starch, and natural folate). However, the study-specific factor loadings presented some differences across each other (Figure 1 right panel, in black box), providing a deeper understanding of the background-specific dietary patterns. In particular, the short-, medium-, long-chain saturated fatty acids and the long-chain monounsaturated fatty acids are more expressed for the Central America pattern than the other background patterns, revealing that the Central America background is more associated with the good oily components. In fact, these nutrients can be found in nuts, seeds, and coconut oil. The Cuban background pattern expressed higher loadings in calcium, phosphorus, and thiamin than the other background groups but not in potassium. This suggests that the Cuban background pattern is enriched with more vegetable source foods than the other background groups. Finally, the Dominican and Mexican background patterns showed higher-valued loadings for the fiber (soluble and insoluble) and not in the pantothenic acid and vitamin B6. This suggests that the Dominican and Mexican background patterns can be associated with grain consumption. The other two background patterns, i.e., Puerto-Rican and South American, are more similar,

representing some variants of an animal profile.

Associations with food groups.

To further corroborate and validate our results, we associate each common and study-specific factor with the food groups from the 24-hour recalls. Thus, we estimate the factor scores, i.e., the degree to which each subject's diet adheres to one of the identified factors. In order to do that, we adopted the Bartlett and Thurstone approaches (Johnson, 1988; DiStefano et al., 2009) in the MSFR model. The correlations between Bartlett and Thurstone scores exceeded 0.95 for the common and study-specific factors, so we adopted the Bartlett method since scores are uncorrelated between each other (DiStefano et al., 2009), see Supplement D for further details. We reported the association between the factors, common and study-specific, and the food group in Figure 5, left and right panels, respectively, where in grey is reported the high consumption of the corresponding food in that factor.

The names attributable to each common factor, i.e., Plant-based food, Animal products, Dairy products, and Seafood, were further confirmed by this analysis. In fact, the Plant-based foods pattern is highly enriched in all types of fruits (Fruit-Citrus, Fruit-Other, Fruit-All) and vegetarian (Dark Green and Veg-Tomatoes). This pattern is also enriched in grain, especially refined and soy, potentially related to the Hispanic diet, with corn, soybean, and tortilla. The Animal products pattern is enriched in Deli-Meat, Organ Meats, Meat-All, Cheese, Dairy Dessert and Milk. The pattern of Dairy products is enriched in all the dairy foods, i.e., Milk, Cheese, Yogurt, Dairy Dessert, and Milk. These last two dietary patterns express a crucial distinction from one another, one more associated with animal fat and animal consumption, the other more oriented on dairy consumption. The Seafood dietary pattern is enriched in Fish but also in Cheese, Dairy dessert. It is the only pattern to be enriched in alcohol consumption.

The study-specific analyses confirm our first visual inspection. All the background patterns reported high meat, red, poultry, and organ meats consumption. Two background patterns, i.e., Puerto-Rican and South American, are similar, with high consumption in all the meat types (including poultry), with some nuances. For example, the Puerto-Rican pattern presents high consumption of alcohol compared to the South Americans. We called Puerto-Rican and South American patterns the “animal source-only” patterns. High consumption of alcohol is also presented in two other background dietary patterns, Central American and Cuban. The Central American pattern is very similar to the “animal source-only” patterns, with some slight differences, i.e., it does not show the deli-meat consumption and is enriched in milk. The Dominican and Mexican patterns present high consumption of grain, especially refined grain and grain-all, revealing these two patterns to be not only animal sources. The Cuban pattern is the only one to show high consumption of vegetables (Dark green) and potatoes together with whole grains. Thus, this pattern is based on vegetable sources.

Association with the Alternative Healthy Eating Index(AHEI-2010).

We further performed an analysis to validate our dietary patterns, associating both the common and the study-specific patterns with the Alternative Healthy Eating Index (AHEI-2010). The AHEI-2010 is a metric to determine if a group of foods, and so nutrients, adheres to the Dietary Guidelines for Americans (DGA)(Chiuve et al., 2012). The alternative eating index was adjusted based on foods and nutrients preventing chronic disease risk. The AHEI-2010 is an 11-component diet quality score ranging from 0 to 110. The higher the AHEI-2010 index, the lower the chronic disease risk. Thus, it is a crucial measure to detect if patterns can be related to any possible risk, especially cardiometabolic disease risk (Liese et al., 2022).

We assessed the association between our dietary patterns and the AHEI-2010 by esti-

imating the mean score within quantile-based categories of factor scores using a weighted generalized linear regression model adjusted for total energy intake only. We computed the mean and the standard error for each estimate (Figure 5). We remark that we have not included any covariates as confounders since we have already accounted for those in our multi-study factor regression model.

For the common dietary patterns, we observed that both the Plant-based foods and the Seafood patterns increased the AHEI-2010, while both the Animal Products and Dairy products patterns decreased the AHEI-2010. The Animal Products pattern is strongly decreasing the AHEI-2010, scoring from 49.7 (first quantile) to 45.2 (fifth quantile), while the Dairy products pattern is slightly decreasing, scoring from 48.1 (first quantile) to 46.7 (fifth quantile).

The study-specific patterns have similar behavior, all decreasing the AHEI, with some differences. For instance, the Dominican background dietary pattern increases strongly the AHEI, ranging from 51.2 (first quantile) to 46.4 (third quantile). The Cuban background dietary pattern associated with more vegetables slightly decreases the AHEI, ranging from 44.7 (first quantile) to 43.5 (third quantile). The standard errors for the study-specific are all very low, close to zero.

6 Discussion

In this article, we aim to identify the shared and ethnic background site-specific dietary patterns in the HCHS/SOL study, while adjusting for socio-demographic characteristics or confounders that do not affect the dietary patterns like: gender, education level and alcohol and cigarette intake and BMI. To achieve this goal, we have presented a novel class of factor models: the Multy-Study Factor Regression (MSFR).

MSFR integrates data from multiple sources using joint dimension reduction, via Multi-study Factor Analyses (De Vito et al., 2019, 2021), and covariate effect adjustment, via latent factor regression (Avalos-Pacheco et al., 2022; Carvalho et al., 2008). Our MSFR is fitted in a deterministic fashion via an efficient ECM algorithm with closed-form updates and publicly available at <https://github.com/rdevito/MSFR>.

Our proposed MSFR has the potential to be adopted in several different data settings where the goal is to disentangle the similarities and dissimilarities among heterogeneous populations, studies or groups, with the added benefit of adjusting for the effects of covariates. The proposed covariate adjustment essentially makes use of information about relationships between socio-demographic characteristics and the outcome so that our MSFR can better identify the common and study-specific loading matrices and latent factors. Furthermore, MSFR had the most robust estimation of factor cardinality (common and study-specific), while our competitors MSFA and FR required a higher number of factors to take into account the covariate effects and the lack of study specific factors, respectively. The unadjusted MSFA provides a competitive estimation of the common and study-specific loadings, in cases when the covariates are weakly prognostic of the outcomes (Scenario 1 of our simulations). However, their inference may suffer in cases with strongly prognostic outcomes (Scenarios 2 and 3 of our simulations). Thus, we recommend the use of our MSFR model generally, regardless of whether our data have a high or low covariate effect.

In our nutritional epidemiology application, we show that the covariate adjustment of our MSFR tends to improve the quality of our estimations and predictions. Further, our model was able to provide interpretable dietary patterns for the whole Hispanic Community, as well as for each Latino ethnic background. Our obtained factors, common and study-specific, were explained and named according to their nutrient values and their correlation to different food groups. Finally, we illustrated the utility of our method in a supervised

framework by studying the factor association with the alternative healthy eating index. We emphasize that our proposed method eliminates the need for an additional covariance adjustment to analyze the AHEI-2010 scores, which is required in the case of MSFA.

We remark that our novel MSFR can be extended to frameworks of interest beyond nutritional epidemiology, such as cancer genomics to identify patterns of common and study-specific transcriptional variation while correcting for pre-treatment patient characteristics, or finance to study common market trends and study-specific recession/expansion periods, while adding other economic variables.

In summary, our model is essential in the case application considered here. We hope it will help the joint analyses of multiple studies in many different settings, abating the current challenges of reproducibility of unsupervised analyses in nutritional epidemiology and data science.

References

- Akaike, H. (1974). A new look at the statistical model identification. *IEEE transactions on automatic control* 19(6), 716–723.
- Aune, D. et al. (2016). Nut consumption and risk of cardiovascular disease, total cancer, all-cause and cause-specific mortality: a systematic review and dose-response meta-analysis of prospective studies. *BMC medicine* 14(1), 1–14.
- Avalos-Pacheco, A. (2018). *Factor regression for dimensionality reduction and data integration techniques with applications to cancer data*. University of Warwick, PhD thesis.
- Avalos-Pacheco, A., D. Rossell, and R. S. Savage (2022). Heterogeneous large datasets integration using Bayesian factor regression. *Bayesian analysis* 17(1), 33–66.

- Bennett, G., L. A. Bardon, and E. R. Gibney (2022). A comparison of dietary patterns and factors influencing food choice among ethnic groups living in one locality: a systematic review. *Nutrients* 14(5), 941.
- Carvalho, C. M. et al. (2008). High-dimensional sparse factor modeling: Applications in gene expression genomics. *Journal of the American Statistical Association* 103(484), 1438–1456.
- Castello, A. et al. (2014). Spanish mediterranean diet and other dietary patterns and breast cancer risk: case–control epigeicam study. *British journal of cancer* 111(7), 1454–1462.
- Castelló, A. et al. (2022). Adherence to the western, prudent and mediterranean dietary patterns and colorectal cancer risk: Findings from the spanish cohort of the european prospective investigation into cancer and nutrition (epic-spain). *Nutrients* 14(15), 3085.
- Chiuve, S. E. et al. (2012). Alternative dietary indices both strongly predict risk of chronic disease. *The Journal of nutrition* 142(6), 1009–1018.
- Conway, D. I. et al. (2009). Enhancing epidemiologic research on head and neck cancer: Inhance-the international head and neck cancer epidemiology consortium. *Oral oncology* 45(9), 743–746.
- Daviglus, M. L., A. Pirzada, and G. A. Talavera (2014). Cardiovascular disease risk factors in the hispanic/latino population: lessons from the hispanic community health study/study of latinos (hchs/sol). *Progress in cardiovascular diseases* 57(3), 230–236.
- De Vito, R. et al. (2019). Shared and study-specific dietary patterns and head and neck cancer risk in an international consortium. *Epidemiology (Cambridge, Mass.)* 30(1), 93.

- De Vito, R. et al. (2022). Shared and ethnic background site-specific dietary patterns in the hispanic community health study/study of latinos (hchs/sol). *medRxiv*, 2022–06.
- De Vito, R., R. Bellio, L. Trippa, and G. Parmigiani (2019). Multi-study factor analysis. *Biometrics* 75(1), 337–346.
- De Vito, R., R. Bellio, L. Trippa, and G. Parmigiani (2021). Bayesian multistudy factor analysis for high-throughput biological data. *The annals of applied statistics* 15(4), 1723–1741.
- DiStefano, C., M. Zhu, and D. Mindrila (2009). Understanding and using factor scores: Considerations for the applied researcher. *Practical Assessment, Research, and Evaluation* 14(1), 20.
- Edefonti, V. et al. (2012). Nutrient-based dietary patterns and the risk of head and neck cancer: a pooled analysis in the international head and neck cancer epidemiology consortium. *Annals of Oncology* 23(7), 1869–1880.
- Foster, G. D. et al. (2003). A randomized trial of a low-carbohydrate diet for obesity. *New England Journal of Medicine* 348(21), 2082–2090.
- Frühwirth-Schnatter, S., D. Hosszejni, and H. F. Lopes (2023). Sparse bayesian factor analysis when the number of factors is unknown.
- GBD 2013 Risk Factors Collaborators and others (2015). Global, regional, and national comparative risk assessment of 79 behavioural, environmental and occupational, and metabolic risks or clusters of risks in 188 countries, 1990–2013: a systematic analysis for the global burden of disease study 2013. *Lancet* 386(10010), 2287.

- Haines, P. S., A. M. Siega-Riz, and B. M. Popkin (1999). The diet quality index revised: a measurement instrument for populations. *Journal of the American Dietetic Association* 99(6), 697–704.
- Hashibe, M. et al. (2007). Alcohol drinking in never users of tobacco, cigarette smoking in never drinkers, and the risk of head and neck cancer: pooled analysis in the international head and neck cancer epidemiology consortium. *Journal of the National Cancer Institute* 99(10), 777–789.
- Islam, M. A. et al. (2019). Trans fatty acids and lipid profile: A serious risk factor to cardiovascular disease, cancer and diabetes. *Diabetes & Metabolic Syndrome: Clinical Research & Reviews* 13(2), 1643–1647.
- Johnson, R. A. R. A. (1988). *Applied multivariate statistical analysis* (2nd ed. ed.). Prentice-Hall series in statistics. Englewood Cliffs, N.J.: Prentice-Hall.
- Kaiser, H. F. (1958). The varimax criterion for analytic rotation in factor analysis. *Psychometrika* 23(3), 187–200.
- Kromhout, D. (2001). Diet and cardiovascular diseases. *The journal of nutrition, health & aging* 5(3), 144–149.
- LaVange, L. M. et al. (2010). Sample design and cohort selection in the Hispanic Community Health Study/Study of Latinos. *Annals of epidemiology* 20(8), 642–649.
- Lichtenstein, A. H. (2003). Dietary fat and cardiovascular disease risk: quantity or quality? *Journal of Women's Health* 12(2), 109–114.
- Liese, A. D. et al. (2015). The dietary patterns methods project: synthesis of findings across cohorts and relevance to dietary guidance. *The Journal of nutrition* 145(3), 393–402.

- Liese, A. D. et al. (2022). Variations in dietary patterns defined by the healthy eating index 2015 and associations with mortality: findings from the dietary patterns methods project. *The Journal of Nutrition* 152(3), 796–804.
- Lopes, H. F. and M. West (2004). Bayesian model assessment in factor analysis. *Statistica Sinica* 14(1), 41–67.
- McLachlan, G. J. (2008). *The EM algorithm and extensions* (2nd ed. ed.). Wiley series in probability and statistics. Hoboken, N.J.: Wiley-Interscience.
- Meng, X.-L. and D. B. Rubin (1993). Maximum likelihood estimation via the ecm algorithm: A general framework. *Biometrika* 80(2), 267–278.
- Morgenstern, O. and M. A. Woodbury (1950). Stability of inverses of input-output matrices. *Econometrica* 18, 190.
- National Heart, Lung, and Blood Institute and others (2009). Hispanic community health study/study of latinos (hchs/sol). *Bethesda, MD: NHLBI*.
- Robert, P. and Y. Escoufier (1976). A unifying tool for linear multivariate statistical methods: The rv- coefficient. *Applied Statistics* 25(3), 257–265.
- Schulze, M. B., K. Hoffmann, A. Kroke, and H. Boeing (2003). An approach to construct simplified measures of dietary patterns from exploratory factor analysis. *British Journal of Nutrition* 89(3), 409–418.
- Schwarz, G. (1978). Estimating the dimension of a model. *The Annals of statistics* 6(2), 461–464.

- Sorlie, P. D. et al. (2010). Design and implementation of the hispanic community health study/study of latinos. *Annals of epidemiology* 20(8), 629–641.
- Stearns, J. C. et al. (2017). Ethnic and diet-related differences in the healthy infant microbiome. *Genome medicine* 9, 1–12.
- Stephenson, B. J., A. H. Herring, and A. Olshan (2020). Robust clustering with subpopulation-specific deviations. *Journal of the American Statistical Association* 115(530), 521–537.
- Trichopoulos, D. et al. (1985). Diet and cancer of the stomach: a case-control study in greece. *International journal of cancer* 36(3), 291–297.
- Tucker, L. A., G. T. Seljaas, and R. L. Hager (1997). Body fat percentage of children varies according to their diet composition. *Journal of the American Dietetic Association* 97(9), 981–986.
- West, M. (2003). *Bayesian factor regression models in the “large p, small n” paradigm*, Volume 7. Elsevier, North-Holland [u.a.].
- Willett, W. C. and B. MacMahon (1984). Diet and cancer-an overview. *New England Journal of Medicine* 310(11), 697–703.
- Yoon, P. W. et al. (2001). The national birth defects prevention study. *Public health reports* 116(Suppl 1), 32.
- Zulyniak, M. A. et al. (2017). Does the impact of a plant-based diet during pregnancy on birth weight differ by ethnicity? a dietary pattern analysis from a prospective canadian birth cohort alliance. *BMJ open* 7(11), e017753.

Figure 1: Heatmap of the common (left panel) and study-specific (right panel) factor loadings in the HCHS/SOL.

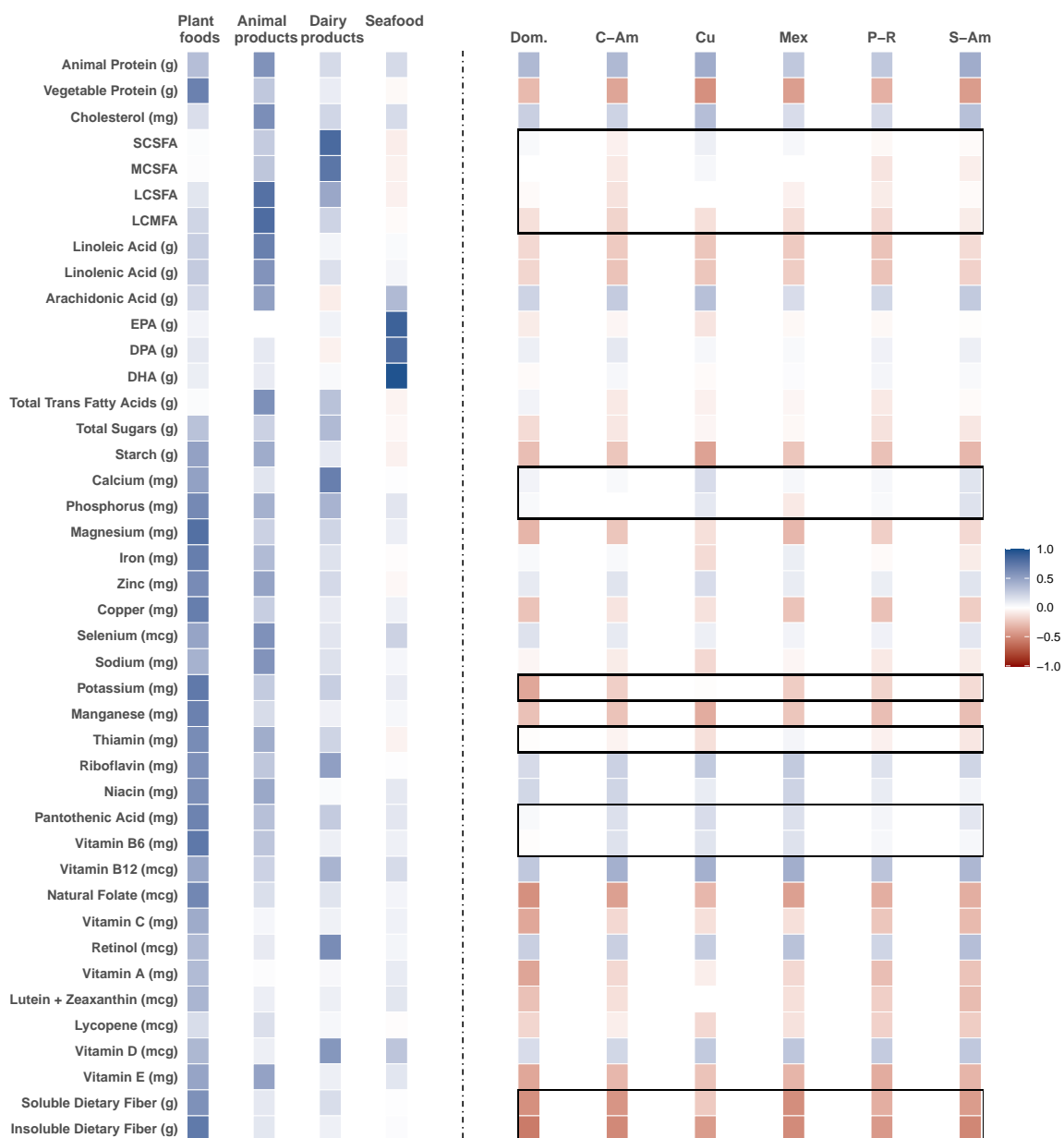


Figure 2: Association of each factor with each food group for each common factor (first box) and each study-specific factor (second box).

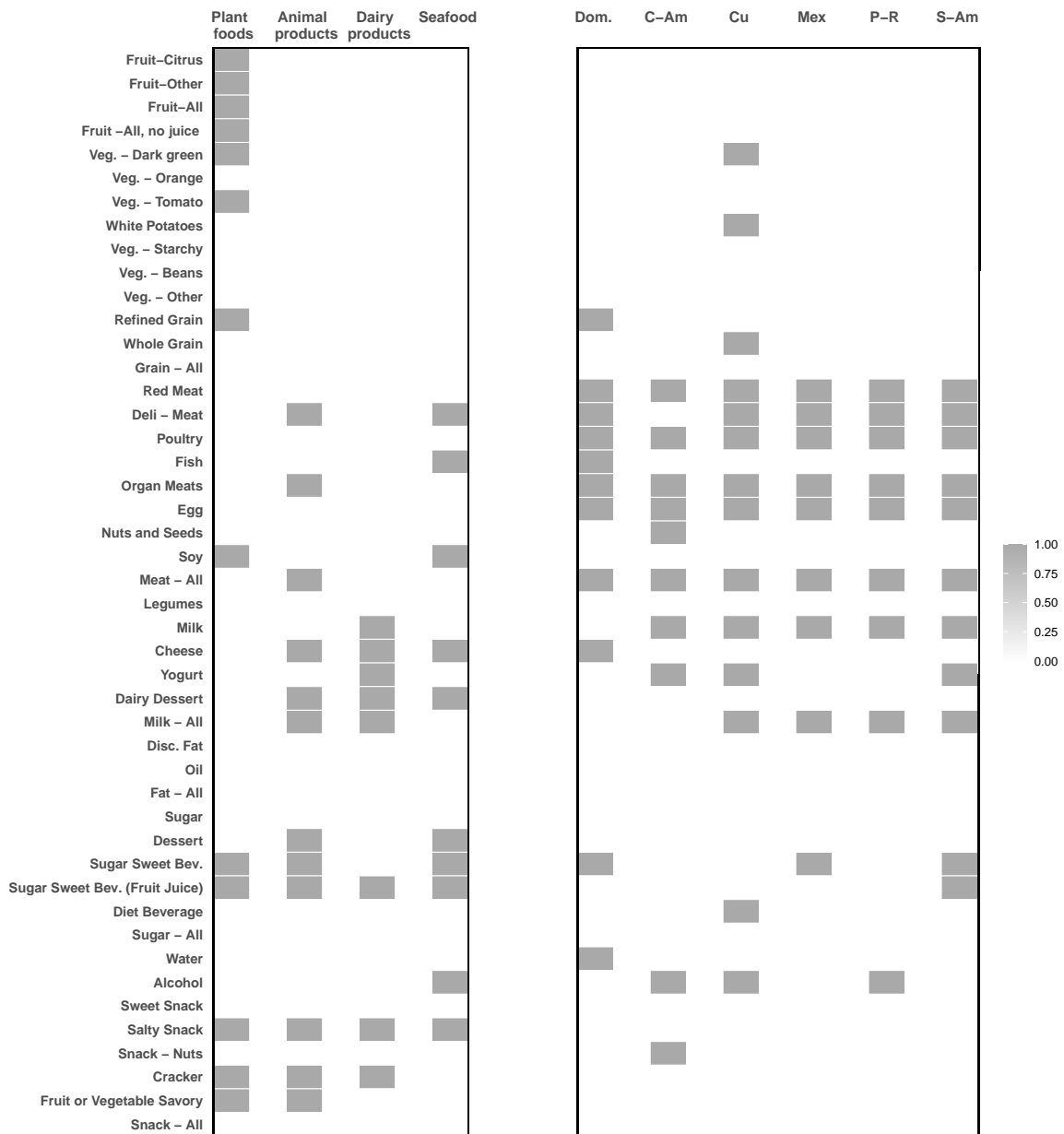
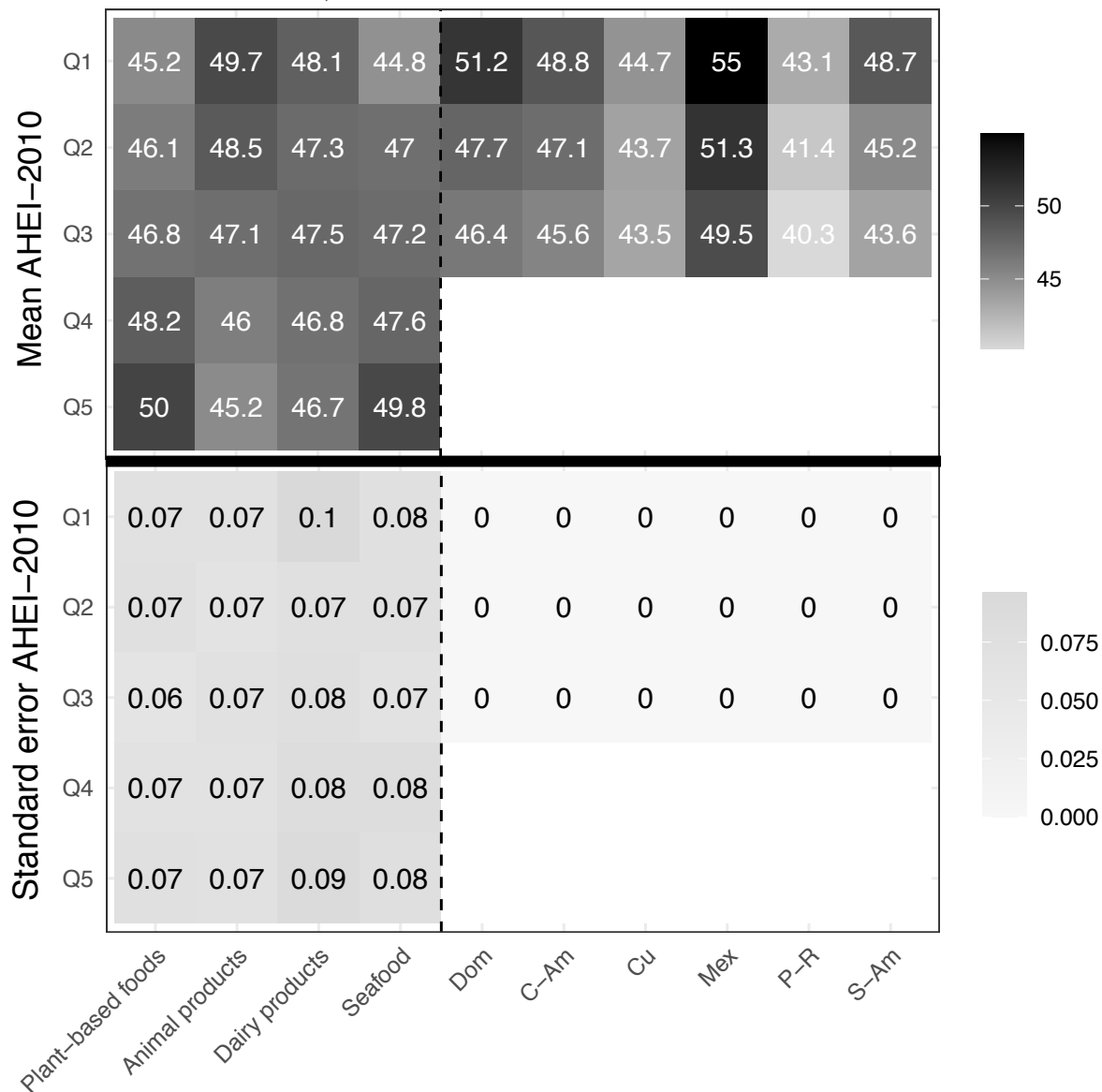


Figure 3: Mean (top panels) association of each factor with the AHEI-2010 and its standard deviation (bottom panels), for both the common (left side of the dashed line) and the study-specific (right side of the dashed line)



Supplementary Materials for

“Multi-study factor regression model: an application in nutritional epidemiology.”

A ECM algorithm

In the E-step, we compute the expectation of the For $s = 1, \dots, S$, $i = 1, \dots, n_s$, and given the parameters $\boldsymbol{\theta} = \{\boldsymbol{\Phi}, \boldsymbol{\Lambda}_s, \boldsymbol{\Psi}_s, \boldsymbol{\beta}\}$, with $\mathbf{b}_{is}, \mathbf{f}_{is}, \mathbf{l}_{is}$ observed, the complete log-likelihood would be:

$$\begin{aligned}
 l_c(\boldsymbol{\theta}) &\propto \sum_{s=1}^S \sum_{i=1}^{n_s} \log (p(\mathbf{x}_{is}|\mathbf{b}_{is}, \mathbf{f}_{is}, \mathbf{l}_{is}, \boldsymbol{\theta})p(\mathbf{f}_{is}|\boldsymbol{\theta})p(\mathbf{l}_{is}|\boldsymbol{\theta})) \\
 &\propto \sum_{s=1}^S \left\{ -\frac{1}{2} \sum_i^{n_s} [\mathbf{x}_{is} - \boldsymbol{\beta}\mathbf{b}_{is} - \boldsymbol{\Phi}\mathbf{f}_{is} - \boldsymbol{\Lambda}_s\mathbf{l}_{is}]^\top \boldsymbol{\Psi}_s^{-1} [\mathbf{x}_{is} - \boldsymbol{\beta}\mathbf{b}_{is} - \boldsymbol{\Phi}\mathbf{f}_{is} - \boldsymbol{\Lambda}_s\mathbf{l}_{is}] \right. \\
 &\quad \left. - \frac{n_s}{2} \log |\boldsymbol{\Psi}_s| \right\} \tag{1}
 \end{aligned}$$

For simplicity let $\tilde{\mathbf{x}}_{is} = \mathbf{x}_{is} - \boldsymbol{\beta}\mathbf{b}_{is}$ (note than we can do that because \mathbf{b}_{is} are really observed, not like the factors).

$$\begin{aligned}
\begin{bmatrix} \mathbf{x}_{is} \\ \mathbf{f}_i \\ \mathbf{l}_{is} \end{bmatrix} &= N \left(\begin{bmatrix} \beta \mathbf{b}_{is} \\ 0 \\ 0 \end{bmatrix}, \begin{bmatrix} \Sigma_s & \Phi & \Lambda_s \\ \Phi^\top & \mathbf{I}_q & 0 \\ \Lambda_s^\top & 0 & \mathbf{I}_{q_s} \end{bmatrix} \right) = \\
\begin{bmatrix} \mathbf{x}_{is} - \beta \mathbf{b}_{is} \\ \mathbf{f}_i \\ \mathbf{l}_{is} \end{bmatrix} &= \begin{bmatrix} \tilde{\mathbf{x}}_{is} \\ \mathbf{f}_i \\ \mathbf{l}_{is} \end{bmatrix} = N \left(\begin{bmatrix} 0 \\ 0 \\ 0 \end{bmatrix}, \begin{bmatrix} \Sigma_s & \Phi & \Lambda_s \\ \Phi^\top & \mathbf{I}_q & 0 \\ \Lambda_s^\top & 0 & \mathbf{I}_{q_s} \end{bmatrix} \right),
\end{aligned} \tag{2}$$

with $\Sigma_s = (\Phi\Phi^\top + \Lambda_s\Lambda_s^\top + \Psi_s)$. Equation (1) can be seen as:

$$\begin{aligned}
l_c(\boldsymbol{\theta}) &= \sum_{s=1}^S \left\{ -\frac{1}{2} \sum_i^{n_s} [\tilde{\mathbf{x}}_{is} - \Phi \mathbf{f}_{is} - \Lambda_s \mathbf{l}_{is}]^\top \Psi_s^{-1} [\tilde{\mathbf{x}}_{is} - \Phi \mathbf{f}_{is} - \Lambda_s \mathbf{l}_{is}] - \frac{n_s}{2} \log |\Psi_s| \right\} \\
&= \sum_{s=1}^S \left\{ -\frac{n_s}{2} \text{tr} \left(\frac{\Psi_s^{-1} \sum_i^{n_s} [\tilde{\mathbf{x}}_{is} - \Phi \mathbf{f}_{is} - \Lambda_s \mathbf{l}_{is}] [\tilde{\mathbf{x}}_{is} - \Phi \mathbf{f}_{is} - \Lambda_s \mathbf{l}_{is}]^\top}{n_s} \right) \right. \\
&\quad \left. - \frac{n_s}{2} \log |\Psi_s| \right\} \\
&= \sum_{s=1}^S \left\{ -\frac{n_s}{2} \log |\Psi_s| \right. \\
&\quad \left. - \frac{n_s}{2} \text{tr} \left[\Psi_s^{-1} \frac{\sum_i^{n_s} (\tilde{\mathbf{x}}_{is} \tilde{\mathbf{x}}_{is}^\top + \Phi \mathbf{f}_{is} \mathbf{f}_{is}^\top \Phi^\top + \Lambda_s \mathbf{l}_{is} \mathbf{l}_{is}^\top \Lambda_s^\top}{n_s} \right. \right. \\
&\quad \left. \left. - \frac{2\tilde{\mathbf{x}}_{is} \mathbf{f}_{is}^\top \Phi^\top - 2\tilde{\mathbf{x}}_{is} \mathbf{l}_{is}^\top \Lambda_s^\top + 2\Phi \mathbf{f}_{is} \mathbf{l}_{is}^\top \Lambda_s^\top}{n_s} \right] \right\}
\end{aligned} \tag{3}$$

Taking the expectations of Equation (3)

$$\begin{aligned}
l_c(\boldsymbol{\theta}) &= \sum_{s=1}^S \left\{ -\frac{n_s}{2} \log |\Psi_s| - \frac{n_s}{2} \text{tr} \left[\Psi_s^{-1} \frac{\sum_i^{n_s} (E[\tilde{\mathbf{x}}_{is} \tilde{\mathbf{x}}_{is}^\top | \tilde{\mathbf{x}}_{is}]}{n_s} \right. \right. \\
&\quad \left. \left. + \frac{\Phi E[\mathbf{f}_{is} \mathbf{f}_{is}^\top | \tilde{\mathbf{x}}_{is}] \Phi^\top + \Lambda_s E[\mathbf{l}_{is} \mathbf{l}_{is}^\top | \tilde{\mathbf{x}}_{is}] \Lambda_s^\top - 2E[\tilde{\mathbf{x}}_{is} \mathbf{f}_{is}^\top | \tilde{\mathbf{x}}_{is}] \Phi^\top}{n_s} \right. \right. \\
&\quad \left. \left. - \frac{2E[\tilde{\mathbf{x}}_{is} \mathbf{l}_{is}^\top | \tilde{\mathbf{x}}_{is}] \Lambda_s^\top + 2\Phi E[\mathbf{f}_{is} \mathbf{l}_{is}^\top | \tilde{\mathbf{x}}_{is}] \Lambda_s^\top}{n_s} \right] \right\}
\end{aligned} \tag{4}$$

The Expectation/Conditional Maximization (ECM) algorithm uses the complete-data likelihood (1) in order to maximize the actual likelihood of the parameters.

The E-step

The expectations of the following quantities

$$\begin{aligned} \mathbf{C}_{\tilde{x}_s \tilde{x}_s} &= \frac{\sum_{i=1}^{n_s} \tilde{\mathbf{x}}_{is} \tilde{\mathbf{x}}_{is}^\top}{n_s}, & \mathbf{C}_{ff} &= \frac{\sum_{i=1}^{n_s} \mathbf{f}_{is} \mathbf{f}_{is}^\top}{n_s}, & \mathbf{C}_{l_s l_s} &= \frac{\sum_{i=1}^{n_s} \mathbf{l}_{is} \mathbf{l}_{is}^\top}{n_s}, \\ \mathbf{C}_{\tilde{x}_s f} &= \frac{\sum_{i=1}^{n_s} \tilde{\mathbf{x}}_{is} \mathbf{f}_{is}^\top}{n_s}, & \mathbf{C}_{\tilde{x}_s l_s} &= \frac{\sum_{i=1}^{n_s} \tilde{\mathbf{x}}_{is} \mathbf{l}_{is}^\top}{n_s}, & \mathbf{C}_{f l_s} &= \frac{\sum_{i=1}^{n_s} \mathbf{f}_{is} \mathbf{l}_{is}^\top}{n_s}, \end{aligned}$$

will be

$$\begin{aligned} \mathbf{T}_{\tilde{x}_s \tilde{x}_s} &= \mathbb{E}[\mathbf{C}_{\tilde{x}_s \tilde{x}_s} | \tilde{\mathbf{x}}_{is}, \boldsymbol{\theta}_{t-1}] = \mathbf{C}_{\tilde{x}_s \tilde{x}_s}, & \mathbf{T}_{ff} &= \mathbb{E}[\mathbf{C}_{ff} | \tilde{\mathbf{x}}_{is}, \boldsymbol{\theta}_{t-1}] = \delta \mathbf{C}_{\tilde{x}_s \tilde{x}_s} \delta^\top + \boldsymbol{\Delta}, \\ \mathbf{T}_{\tilde{x}_s l_s} &= \mathbb{E}[\mathbf{C}_{\tilde{x}_s l_s} | \tilde{\mathbf{x}}_{is}, \boldsymbol{\theta}_{t-1}] = \mathbf{C}_{\tilde{x}_s l_s}, & \mathbf{T}_{l_s l_s} &= \mathbb{E}[\mathbf{C}_{l_s l_s} | \tilde{\mathbf{x}}_{is}, \boldsymbol{\theta}_{t-1}] = \delta_s \mathbf{C}_{\tilde{x}_s \tilde{x}_s} \delta_s^\top + \boldsymbol{\Delta}_s, \\ \mathbf{T}_{\tilde{x}_s f} &= \mathbb{E}[\mathbf{C}_{\tilde{x}_s f} | \tilde{\mathbf{x}}_{is}, \boldsymbol{\theta}_{t-1}] = \mathbf{C}_{\tilde{x}_s f}, & \mathbf{T}_{f l_s} &= \mathbb{E}[\mathbf{C}_{f l_s} | \tilde{\mathbf{x}}_{is}, \boldsymbol{\theta}_{t-1}] = \delta \mathbf{C}_{\tilde{x}_s \tilde{x}_s} \delta_s^\top + \boldsymbol{\Delta}_{fl}. \end{aligned}$$

where

$$\boldsymbol{\Delta}_{fl} = \text{Cov}[\mathbf{l}_{is}, \mathbf{f}_{is} | \tilde{\mathbf{x}}_{is}, \boldsymbol{\theta}_{t-1}] = \boldsymbol{\Phi}^\top \boldsymbol{\Sigma}_s^{-1} \boldsymbol{\Lambda}_s$$

and

$$\begin{aligned} \delta &= \boldsymbol{\Phi}^\top \boldsymbol{\Sigma}_s^{-1}, & \boldsymbol{\Delta} &= \text{Var}[\mathbf{f}_{is} | \tilde{\mathbf{x}}_{is}, \boldsymbol{\theta}_{t-1}] = \mathbf{I}_q - \boldsymbol{\Phi}^\top \boldsymbol{\Sigma}_s^{-1} \boldsymbol{\Phi}, \\ \delta_s &= \boldsymbol{\Lambda}_s^\top \boldsymbol{\Sigma}_s^{-1}, & \boldsymbol{\Delta}_s &= \text{Var}[\mathbf{l}_{is} | \tilde{\mathbf{x}}_{is}, \boldsymbol{\theta}_{t-1}] = \mathbf{I}_{q_s} - \boldsymbol{\Lambda}_s^\top \boldsymbol{\Sigma}_s^{-1} \boldsymbol{\Lambda}_s. \end{aligned}$$

So we can write the expectation of the complete log-likelihood:

$$\begin{aligned} Q(\boldsymbol{\theta}) &= \sum_{s=1}^S \left(-\frac{n_s}{2} \log |\boldsymbol{\Psi}_s| - \frac{n_s}{2} \text{tr} \left[\boldsymbol{\Psi}_s^{-1} \left(\mathbf{C}_{\tilde{x}_s \tilde{x}_s} + \boldsymbol{\Phi} \mathbf{T}_{ff} \boldsymbol{\Phi}^\top \right. \right. \right. \\ &\quad \left. \left. \left. + \boldsymbol{\Lambda}_s \mathbf{T}_{l_s l_s} \boldsymbol{\Lambda}_s^\top - 2\mathbf{T}_{\tilde{x}_s f} \boldsymbol{\Phi}^\top - 2\mathbf{T}_{\tilde{x}_s l_s} \boldsymbol{\Lambda}_s^\top + 2\boldsymbol{\Phi} \mathbf{T}_{f l_s} \boldsymbol{\Lambda}_s^\top \right) \right] \right) \end{aligned} \quad (5)$$

The CM-step

1. CM1: starting with the update of the error covariance matrix $\boldsymbol{\Psi}_s$ keeping the other parametres at their initial values
2. CM2: update $\boldsymbol{\Phi}$ keeping $\boldsymbol{\Lambda}_s$ at their initial values and $\boldsymbol{\Psi}_s$ at their CM1 values
3. CM3: update $\boldsymbol{\Lambda}_s$ keeping $\boldsymbol{\Phi}$ at the CM2 value and $\boldsymbol{\Psi}_s$ at their CM1 values.

4. CM4: update β keeping $\mathbf{\Lambda}$, $\mathbf{\Phi}$ and $\mathbf{\Psi}_s$ at their CM3, CM2 and CM1 values respectively.

We estimate the matrix $\mathbf{\Psi}_s$ through its inverse, setting

$$\begin{aligned} \frac{\partial Q}{\partial \mathbf{\Psi}_s^{-1}} &= \frac{n_s}{2} \mathbf{\Psi}_s - \frac{n_s}{2} \left(C_{\tilde{x}_s \tilde{x}_s} + \mathbf{\Phi} T_{ff} \mathbf{\Phi}^\top + \mathbf{\Lambda}_s T_{l_s l_s} \mathbf{\Lambda}_s^\top - 2T_{\tilde{x}_s f} \mathbf{\Phi}^\top \right. \\ &\quad \left. - 2T_{\tilde{x}_s f} \mathbf{\Lambda}_s^\top + 2\mathbf{\Phi} T_{f l_s} \mathbf{\Lambda}_s^\top \right) = 0 \end{aligned}$$

and using the diagonal constraint:

$$\tilde{\mathbf{\Psi}}_s = \text{diag} \left\{ C_{\tilde{x}_s \tilde{x}_s} + \mathbf{\Phi} T_{ff} \mathbf{\Phi}^\top + \mathbf{\Lambda}_s T_{l_s l_s} \mathbf{\Lambda}_s^\top - 2T_{\tilde{x}_s f} \mathbf{\Phi}^\top - 2T_{\tilde{x}_s l_s} \mathbf{\Lambda}_s^\top + 2\mathbf{\Phi} T_{f l_s} \mathbf{\Lambda}_s^\top \right\}$$

To maximize $\mathbf{\Phi}$ we compute

$$\frac{\partial Q}{\partial \mathbf{\Phi}} = \sum_{s=1}^S \left(-\frac{n_s}{2} \left(2\tilde{\mathbf{\Psi}}_s^{-1} \mathbf{\Phi} T_{ff} - 2\tilde{\mathbf{\Psi}}_s^{-1} T_{\tilde{x}_s f} + 2\tilde{\mathbf{\Psi}}_s^{-1} \mathbf{\Lambda}_s T_{l_s f}^\top \right) \right) = 0,$$

obtaining

$$\sum_{s=1}^S (n_s \tilde{\mathbf{\Psi}}_s^{-1} \mathbf{\Phi} T_{ff}) = \sum_{s=1}^S (n_s \tilde{\mathbf{\Psi}}_s^{-1} T_{\tilde{x}_s f} - n_s \tilde{\mathbf{\Psi}}_s^{-1} \mathbf{\Lambda}_s T_{f l_s}^\top)$$

To solve this linear equation we use the Lyapunov Equation and we obtain

$$\text{vec}(\tilde{\mathbf{\Phi}}) = \sum_{s=1}^S \left(\mathbf{T}_{ff}^\top \otimes n_s \tilde{\mathbf{\Psi}}_s^{-1} \right) \text{vec} \left(n_s \tilde{\mathbf{\Psi}}_s^{-1} \mathbf{T}_{\tilde{x}_s f} - n_s \tilde{\mathbf{\Psi}}_s^{-1} \mathbf{\Lambda}_s \mathbf{T}_{f l_s}^\top \right).$$

where \otimes is the Kronecker product, vec is the vec operator and the linear equation is solved with the Lyapunov Equation.

To estimate the factor loadings related to the specific factor for the study a , we set

$$\frac{\partial Q}{\partial \Lambda_s} = -\frac{n_s}{2} \tilde{\Psi}_s^{-1} \left(2\Lambda_s T_{l_s l_s} - 2T_{x_s f} + 2\tilde{\Phi} T_{f l_s} \right) = 0$$

obtaining

$$\tilde{\Lambda}_s = \left(T_{x_s f} - \tilde{\Phi} T_{f l_s} \right) \left(T_{l_s l_s} \right)^{-1} \quad (6)$$

Finally we estimate the coefficients of the known covariates, expanding Equation (3) and taking only the part containing $\tilde{\mathbf{x}}_{is}$, we obtain

$$\begin{aligned} Q &\propto \sum_{s=1}^S \left\{ -\frac{n_s}{2} \text{tr} \left[\Psi_s^{-1} \frac{\sum_i^{n_s} ((\mathbf{x}_{is} - \beta \mathbf{b}_{is})(\mathbf{x}_{is} - \beta \mathbf{b}_{is})^\top)}{n_s} \right. \right. \\ &\quad \left. \left. - \frac{2(\mathbf{x}_{is} - \beta \mathbf{b}_{is}) \mathbf{f}_{is}^\top \Phi^\top - 2(\mathbf{x}_{is} - \beta \mathbf{b}_{is}) \mathbf{l}_{is}^\top \Lambda_s^\top}{n_s} \right] \right\} \\ &\propto \sum_{s=1}^S \left\{ -\frac{n_s}{2} \text{tr} \left[\Psi_s^{-1} \frac{\sum_i^{n_s} (-2\mathbf{x}_{is} \mathbf{b}_{is}^\top \beta^\top + \beta \mathbf{b}_{is} \mathbf{b}_{is}^\top \beta^\top)}{n_s} \right. \right. \\ &\quad \left. \left. + \frac{2\beta \mathbf{b}_{is} \mathbf{f}_{is}^\top \Phi^\top + 2\beta \mathbf{b}_{is} \mathbf{l}_{is}^\top \Lambda_s^\top}{n_s} \right] \right\} \end{aligned} \quad (7)$$

Taking the derivative and the expected values of Equation (7)

$$\begin{aligned} \frac{\partial Q}{\partial \beta} &= \sum_{s=1}^S \left(-\frac{n_s}{2} \Psi_s^{-1} \left[\frac{\sum_i^{n_s} 2(\beta \mathbf{b}_{is} \mathbf{b}_{is}^\top - (\mathbf{x}_{is} - \Phi E[\mathbf{f}_{is} | \tilde{\mathbf{x}}_{is}]) \mathbf{b}_{is}^\top)}{n_s} \right. \right. \\ &\quad \left. \left. - \frac{\Lambda_s E[\mathbf{l}_{is} | \tilde{\mathbf{x}}_{is}] \mathbf{b}_{is}^\top}{n_s} \right] \right) = 0 \end{aligned} \quad (8)$$

Solving Equation (8) we obtain:

$$\tilde{\beta} = \left[\sum_{s=1}^S \sum_i^{n_s} (\mathbf{x}_{is} - \tilde{\Phi} E[\mathbf{f}_{is} | \tilde{\mathbf{x}}_{is}] - \tilde{\Lambda}_s E[\mathbf{l}_{is} | \tilde{\mathbf{x}}_{is}]) \mathbf{b}_{is}^\top \right] \left[\sum_{s=1}^S \sum_i^{n_s} (\mathbf{b}_{is} \mathbf{b}_{is}^\top) \right]^{-1} \quad (9)$$

We now need to compute $E[\mathbf{f}_{is}|\tilde{\mathbf{x}}_{is}]$ and $E[\mathbf{l}_{is}|\tilde{\mathbf{x}}_{is}]$, the conditionals from Equation (2) are

$$\begin{aligned} E[\mathbf{f}_{is}|\tilde{\mathbf{x}}_{is}] &= \Phi^\top \Sigma_s^{-1} \tilde{\mathbf{x}}_{is} = \Phi^\top (\Phi \Phi^\top + \Lambda_s \Lambda_s^\top + \Psi_s)^{-1} (\mathbf{x}_{is} - \beta \mathbf{b}_{is}) \\ E[\mathbf{l}_{is}|\tilde{\mathbf{x}}_{is}] &= \Lambda_s^\top \Sigma_s^{-1} \tilde{\mathbf{x}}_{is} = \Lambda_s^\top (\Phi \Phi^\top + \Lambda_s \Lambda_s^\top + \Psi_s)^{-1} (\mathbf{x}_{is} - \beta \mathbf{b}_{is}) \end{aligned} \quad (10)$$

Using the Woodbury identity Equation 10 we obtain

$$\begin{aligned} E[\mathbf{f}_{is}|\tilde{\mathbf{x}}_{is}] &= (\mathbf{I}_q + \Phi^\top (\Lambda_s \Lambda_s^\top + \Psi_s)^{-1} \Phi)^{-1} \Phi^\top (\Lambda_s \Lambda_s^\top + \Psi_s)^{-1} \tilde{\mathbf{x}}_{is} \\ E[\mathbf{l}_{is}|\tilde{\mathbf{x}}_{is}] &= (\mathbf{I}_{q_s} + \Lambda_s^\top (\Phi \Phi^\top + \Psi_s)^{-1} \Lambda_s)^{-1} \Lambda_s^\top (\Phi \Phi^\top + \Psi_s)^{-1} \tilde{\mathbf{x}}_{is} \end{aligned} \quad (11)$$

applying Woodbury identity to $(\Lambda_s \Lambda_s^\top + \Psi_s)^{-1}$ and $(\Phi \Phi^\top + \Psi_s)^{-1}$ we get

$$\begin{aligned} (\Lambda_s \Lambda_s^\top + \Psi_s)^{-1} &= \Psi_s^{-1} - \Psi_s^{-1} \Lambda_s (\mathbf{I}_{q_s} + \Lambda_s^\top \Psi_s^{-1} \Lambda_s)^{-1} \Lambda_s^\top \Psi_s^{-1} \\ (\Phi \Phi^\top + \Psi_s)^{-1} &= \Psi_s^{-1} - \Psi_s^{-1} \Phi (\mathbf{I}_q + \Phi^\top \Psi_s^{-1} \Phi)^{-1} \Phi^\top \Psi_s^{-1} \end{aligned} \quad (12)$$

B Simulation results, models selected via AIC criterion

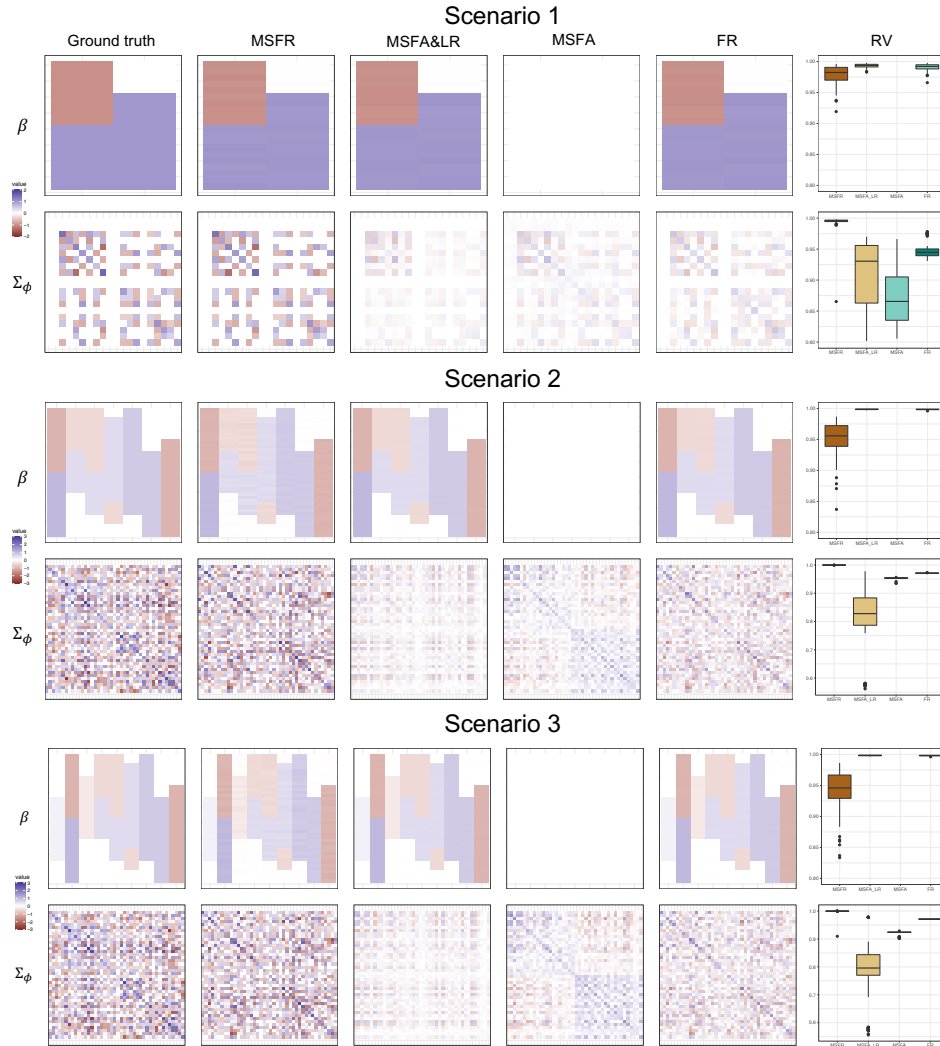


Figure S1: Heatmaps of the average values over 100 simulations, models selected via AIC criterion

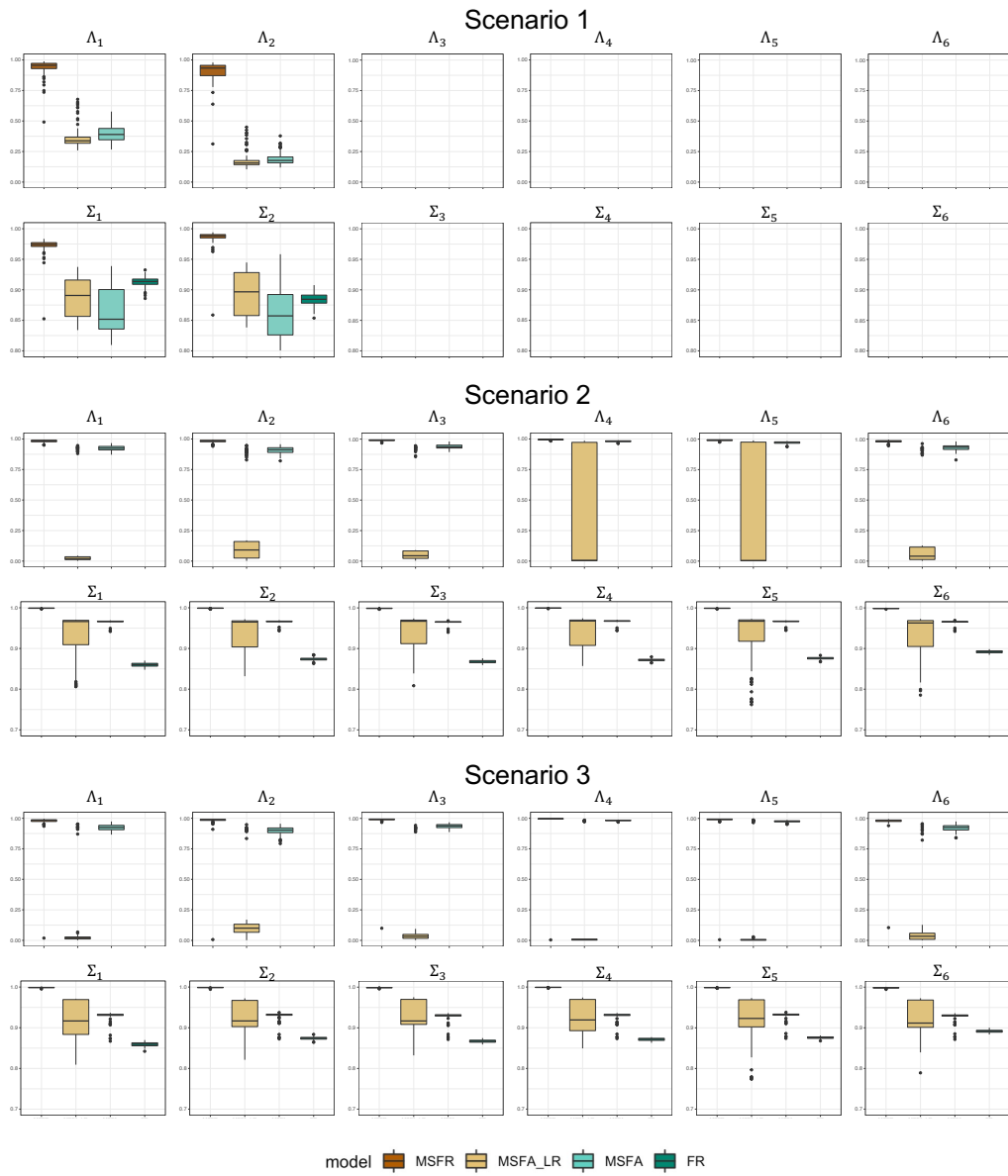


Figure S2: Boxplots of the RV values of 100 simulations, models selected via AIC criterion

C Simulation results, models selected via BIC criterion

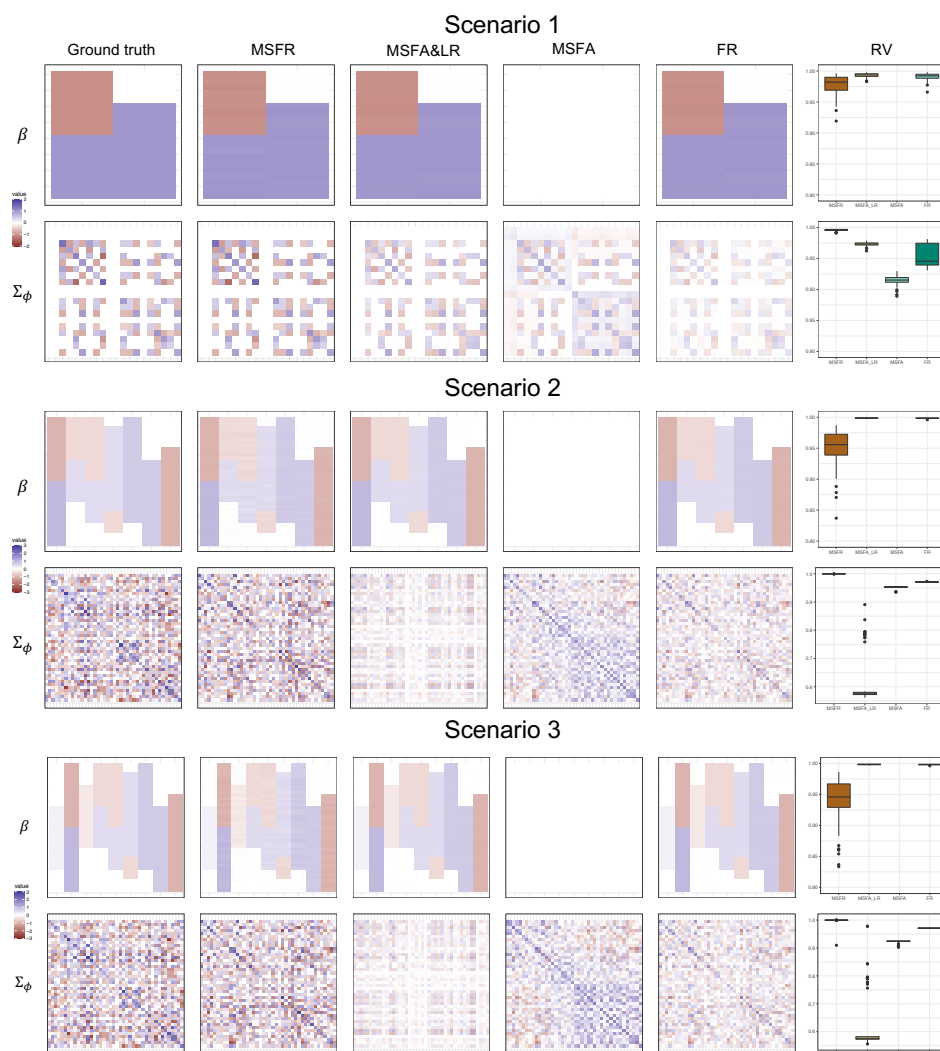


Figure S3: Heatmaps of the average values over 100 simulations, models selected via BIC criterion

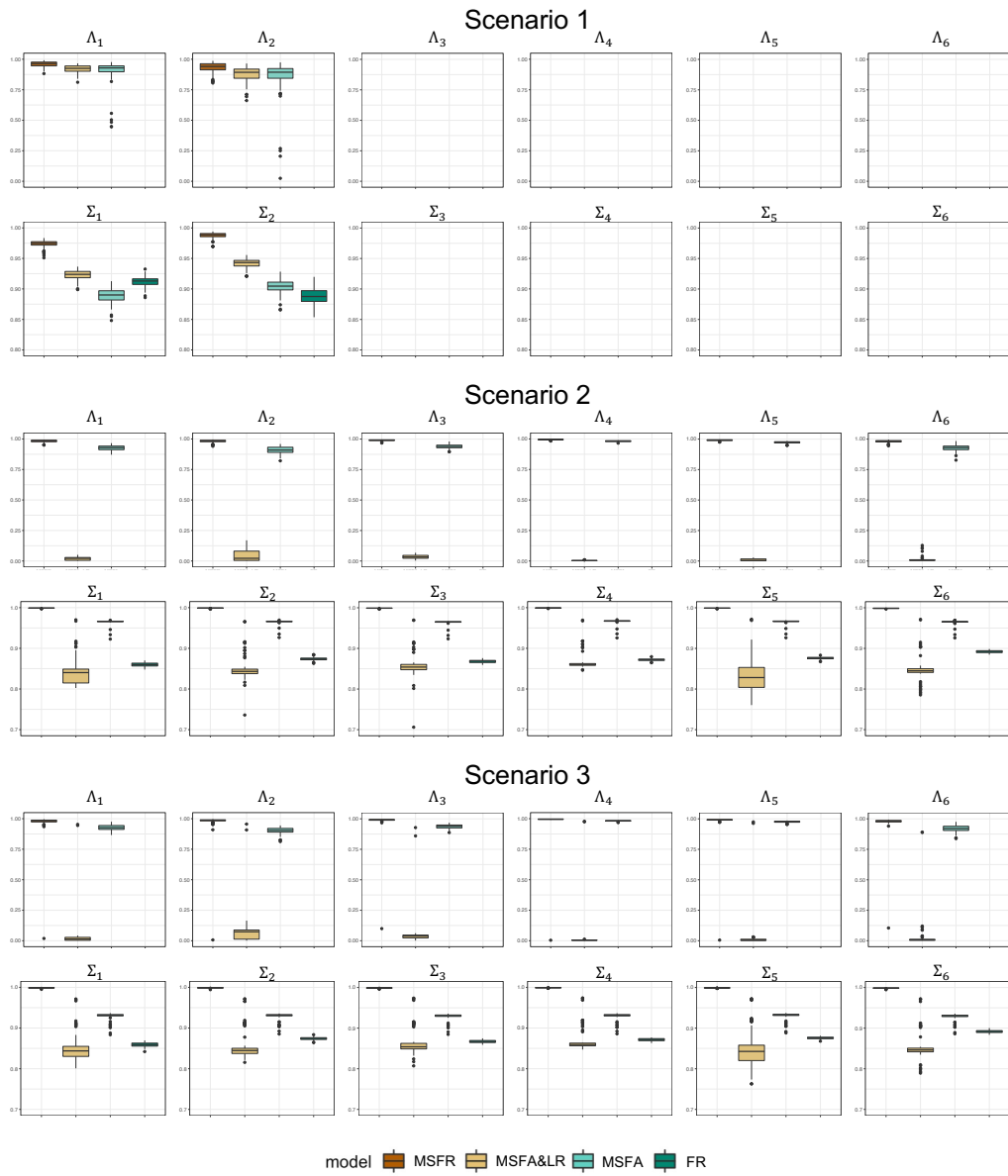


Figure S4: Boxplots of the RV values of 100 simulations, models selected via BIC criterion

D Common and study-specific factor scores

In order to validate associate each factor with the food groups from the 24-hour recalls, we estimate the Bartlett method to compute factor scores, i.e. the degree to which each subject’s diet adheres to one of the identified factor.

We first divided each common factor score in quintile’s categories. We then used these quantile-based categories to validate each estimated factor against each food group provided by HCHS/SOL. We performed a generalized linear regression model adjusted for total energy intake (the only covariate missing from our multi-study regression model). We then predicted from this model the mean of food groups within quantile-based categories. The overall HCHS/SOL mean was calculated for the same food groups as the mean in the merged dataset. We expressed the deviation of the food group intake to its overall or EBS-specific mean as:

$$100 \times \frac{\text{adjusted mean within quintile-based category}}{\text{overall (HCHS/SOL) mean}}.$$

Therefore, if the consumption of a food group exceeded 100%, it indicated that individuals from that factor score quantile category were characterized by high consumption of that food group, compared with the HCHS/SOL overall (for each shared factor).

As for the common factor loadings, we checked the correlation between the Thurstone and the Bartlett method. The correlation between the factor score computed by the two methods is always greater than 0.92, so we decided to adopt the Bartlett method again. We proceeded by dividing each study-specific factor score in tertile’s categories. For the study-specific, we choose the tertile for the sample size. We then used the same procedure adopted for the common factors, so tertile-based categories are computed to validate each estimated factor against each food group provided by HCHS/SOL. We performed a generalized linear regression model adjusted for total energy intake. We then predicted from this model the mean of food groups within the tertile-based categories. The overall means for the study-specific were calculated as the mean of that food group in each background-specific combination. We expressed the deviation of the food group intake to its overall or EBS-specific mean as:

$$100 \times \frac{\text{adjusted mean within tertile-based category}}{\text{background-specific mean}}.$$

Therefore, if the consumption of a food group exceeded 100%, it indicated that individuals from that factor score quantile category were characterized by high consumption of that food group, compared with the background-specific.

E Proofs and Details

E.1 Some others distribution properties

$$\mathbf{f}_a | \mathbf{X}_a \sim \mathbf{N}(\Lambda_a^t \Sigma_A^{-1} x_{ai}; \mathbf{I}_{ka} - \Lambda_a^t \Sigma_A^{-1} \Lambda_a)$$

and

$$\mathbf{f}_c | \mathbf{X}_a \sim \mathbf{N}(\Lambda_c^t \Sigma_A^{-1} x_{ai}; \mathbf{I}_k - \Lambda_c^t \Sigma_A^{-1} \Lambda_c)$$

E.2 Properties for the trace of a square matrix

RESULT from Applied multivariate statistical analysis, Johnson and Wichern pg 168

Let \mathbf{A} be a $k \times k$ symmetric matrix and \mathbf{x} be a $k \times 1$ vector. Then

1. $\mathbf{x}^t \mathbf{A} \mathbf{x} = tr(\mathbf{x}^t \mathbf{A} \mathbf{x}) = tr(\mathbf{A} \mathbf{x} \mathbf{x}^t)$
2. $tr \mathbf{A} = \sum_{i=1}^k \lambda_i$ where λ_i are the eigenvalues of \mathbf{A}

E.3 Kronecker and Vec Operator

The Kronecker Product

The Kronecker product of an $m \times n$ matrix \mathbf{A} and an $r \times q$ matrix \mathbf{B} , is an $mr \times nq$ matrix, $\mathbf{A} \otimes \mathbf{B}$ defined as

$$\mathbf{A} \otimes \mathbf{B} = \begin{bmatrix} A_{11} \mathbf{B} & A_{12} \mathbf{B} & \dots & A_{1n} \mathbf{B} \\ A_{21} \mathbf{B} & A_{22} \mathbf{B} & \dots & A_{2n} \mathbf{B} \\ \vdots & & & \vdots \\ A_{m1} \mathbf{B} & A_{m2} \mathbf{B} & \dots & A_{mn} \mathbf{B} \end{bmatrix}$$

The vec-operator

The vec-operator applied on a matrix \mathbf{A} stacks the columns into a vector, i.e. for a 2×2 matrix

$$\mathbf{A} = \begin{bmatrix} A_{11} & A_{12} \\ A_{21} & A_{22} \end{bmatrix} \quad \text{vec}(\mathbf{A}) = \begin{bmatrix} A_{11} \\ A_{12} \\ A_{21} \\ A_{22} \end{bmatrix}$$

The Lyapunov Equation

$$\mathbf{A}\mathbf{X} + \mathbf{X}\mathbf{B} = \mathbf{C} \quad (13)$$

$$\text{vec}(\mathbf{X}) = (\mathbf{I} \otimes \mathbf{A} + \mathbf{B}^t \otimes \mathbf{I})^{-1} \text{vec}(\mathbf{C}) \quad (14)$$

E.4 The Woodbury identity

$$\begin{aligned} (\mathbf{A} + \mathbf{C}\mathbf{B}\mathbf{C}^\top)^{-1} &= \mathbf{A}^{-1} - \mathbf{A}^{-1}\mathbf{C}(\mathbf{B}^{-1} + \mathbf{C}^\top\mathbf{A}^{-1}\mathbf{C})^{-1}\mathbf{C}^\top\mathbf{A}^{-1} \\ (\mathbf{A} + \mathbf{U}\mathbf{B}\mathbf{V})^{-1} &= \mathbf{A}^{-1} - \mathbf{A}^{-1}\mathbf{U}(\mathbf{B}^{-1} + \mathbf{V}\mathbf{A}^{-1}\mathbf{U})^{-1}\mathbf{V}\mathbf{A}^{-1} \end{aligned} \quad (15)$$

If \mathbf{P} , \mathbf{R} are positive definite, then

$$(\mathbf{P}^{-1} + \mathbf{B}^\top\mathbf{R}^{-1}\mathbf{B})^{-1}\mathbf{B}^\top\mathbf{R}^{-1} = \mathbf{P}\mathbf{B}^\top(\mathbf{B}\mathbf{P}\mathbf{B}^\top + \mathbf{R})^{-1} \quad (16)$$

MSFR expecting values

We now need to compute $E[\mathbf{f}_{is}|\tilde{\mathbf{x}}_{is}]$ and $E[\mathbf{l}_{is}|\tilde{\mathbf{x}}_{is}]$, the conditionals from Equation (2) are

$$\begin{aligned} E[\mathbf{f}_{is}|\tilde{\mathbf{x}}_{is}] &= \Phi^\top \Sigma_s^{-1} \tilde{\mathbf{x}}_{is} = \Phi^\top (\Phi\Phi^\top + \Lambda_s\Lambda_s^\top + \Psi_s)^{-1} (\mathbf{x}_{is} - \beta\mathbf{b}_{is}) \\ E[\mathbf{l}_{is}|\tilde{\mathbf{x}}_{is}] &= \Lambda_s^\top \Sigma_s^{-1} \tilde{\mathbf{x}}_{is} = \Lambda_s^\top (\Phi\Phi^\top + \Lambda_s\Lambda_s^\top + \Psi_s)^{-1} (\mathbf{x}_{is} - \beta\mathbf{b}_{is}) \end{aligned} \quad (17)$$

Using the Woodbury identity Equation (17) we obtain

$$\begin{aligned} E[\mathbf{f}_{is}|\tilde{\mathbf{x}}_{is}] &= (\mathbf{I}_q + \Phi^\top (\Lambda_s\Lambda_s^\top + \Psi_s)^{-1} \Phi)^{-1} \Phi^\top (\Lambda_s\Lambda_s^\top + \Psi_s)^{-1} \tilde{\mathbf{x}}_{is} \\ E[\mathbf{l}_{is}|\tilde{\mathbf{x}}_{is}] &= (\mathbf{I}_{q_s} + \Lambda_s^\top (\Phi\Phi^\top + \Psi_s)^{-1} \Lambda_s)^{-1} \Lambda_s^\top (\Phi\Phi^\top + \Psi_s)^{-1} \tilde{\mathbf{x}}_{is} \end{aligned} \quad (18)$$

applying Woodbury identity to $(\Lambda_s\Lambda_s^\top + \Psi_s)^{-1}$ and $(\Phi\Phi^\top + \Psi_s)^{-1}$ we get

$$\begin{aligned} (\Lambda_s\Lambda_s^\top + \Psi_s)^{-1} &= \Psi_s^{-1} - \Psi_s^{-1}\Lambda_s(\mathbf{I}_{q_s} + \Lambda_s^\top\Psi_s^{-1}\Lambda_s)^{-1}\Lambda_s^\top\Psi_s^{-1} \\ (\Phi\Phi^\top + \Psi_s)^{-1} &= \Psi_s^{-1} - \Psi_s^{-1}\Phi(\mathbf{I}_q + \Phi^\top\Psi_s^{-1}\Phi)^{-1}\Phi^\top\Psi_s^{-1} \end{aligned} \quad (19)$$